

BEYOND THE EXPLORATION-EXPLOITATION TRADE-OFF: A HIDDEN STATE APPROACH FOR LLM REASONING IN RLVR

Fanding Huang^{1*}, Guanbo Huang^{1*}, Xiao Fan¹, Yi He¹, Xiao Liang², Xiao Chen¹,
Qinting Jiang¹, Faisal Nadeem Khan¹, Jingyan Jiang^{3†}, Zhi Wang^{1†}

¹Tsinghua Shenzhen International Graduate School, Tsinghua University

²University of California, Los Angeles ³Shenzhen Technology University

ABSTRACT

A prevailing view in Reinforcement Learning for Verifiable Rewards (RLVR) interprets recent progress through the lens of an exploration-exploitation trade-off, a perspective largely shaped by token-level metrics. We re-examine this perspective, proposing that this perceived trade-off may not be a fundamental constraint but rather an artifact of the measurement level. To investigate this, we shift the analysis to the semantically rich hidden-state space, adopting Effective Rank (ER) to quantify exploration and proposing its novel first- and second-order derivatives, named Effective Rank Velocity (ERV) and Effective Rank Acceleration (ERA), to capture exploitation dynamics. Our analysis reveals that at the hidden-state level, exploration and exploitation could be *decoupled* (Sec. 4). This finding reveals an opportunity to enhance both capacities simultaneously. This insight motivates our method, Velocity-Exploiting Rank-Learning (VERL), the *first* to operationalize the principle of synergistic exploration-exploitation enhancement by directly shaping the RL advantage function. The key innovation is leveraging the theoretically stable ERA as a predictive meta-controller to create a synergistic, dual-channel incentive structure. Instead of forcing a trade-off, VERL prospectively amplifies rewards for exploration to preempt overconfidence and reinforces exploitative gains to consolidate reasoning. Experiments across diverse LLMs and reasoning benchmarks show consistent gains, including up to 21.4% absolute accuracy improvement on the challenging Gaokao 2024 dataset.

 **Code** <https://github.com/hf618/VERL.git>

 **Project** <https://hf618.github.io/VERL.github.io>

1 INTRODUCTION

Recent advancements in Reinforcement Learning with Verifiable Rewards (RLVR) have significantly improved the reasoning abilities of Large Language Models (LLMs). A dominant narrative emerging from these recent works (Chen et al., 2025b; Yue et al., 2025; Deng et al., 2025) interprets this progress through the lens of balancing *exploration* (searching for diverse reasoning paths) and *exploitation* (refining the most promising known strategies). However, this paradigm is almost exclusively rooted in a token-level analysis, where exploration is captured by high-entropy token distributions and exploitation by high-confidence, low-entropy ones. This has inevitably led to the widespread assumption of an inherent trade-off between the two, as a model’s output distribution is seen as unable to be simultaneously uniform and sharp (Agarwal et al., 2025).

This token-centric viewpoint, while convenient, introduces significant limitations. Equating exploration with mere token-level entropy faces an intrinsic dilemma (Fu et al., 2025; Qiao et al., 2025; Agarwal et al., 2025): excessively high entropy risks generating incoherent noise, while overly low entropy stifles exploration it aims to encourage. Similarly, defining exploitation via hand-crafted

*Equal contribution.

†Corresponding authors: Jingyan Jiang and Zhi Wang.

✉ jiangjingyan@sztu.edu.cn; wangzhi@sz.tsinghua.edu.cn

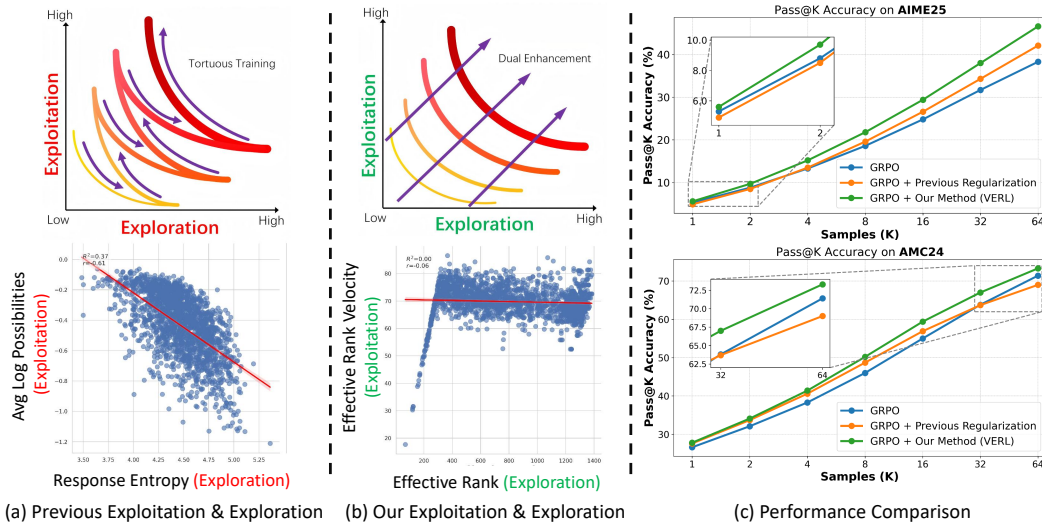


Figure 1: Comparative analysis with the responses of DeepSeek-R1-Distill-Qwen-7B in simpleRL test dataset (Zeng et al., 2025). (a) Traditional metrics for exploitation & exploration are constrained by negative coupling, leading to meandering progress for both capabilities. (b) Our metrics are mutually independent. (c) Training regularization with our metrics demonstrates stronger performance in both exploitation (small K) and exploration (large K).

heuristic rewards (Chen et al., 2025a; Li et al., 2025a; Bensal et al., 2025) produces brittle models with poor generalizability as they simply learn to chase surface-level proxies. More related works in Sec. 7. While many works are aware to consider both exploration and exploitation as in Fig. 1a, their continued reliance on token-level metrics invariably traps them in a cycle of “balancing” the trade-off, instead of doubting its existence. This raises a critical question: *Is the exploration–exploitation trade-off intrinsic to reasoning, or merely an artifact of token-level measurement?*

To answer this, we move beyond token-level statistics to investigate exploration and exploitation at the more granular hidden states level. To analyze these dynamics, we are the first to apply Effective Rank (ER) in an RL context, and take it to quantify exploration by measuring the semantic diversity of hidden-state representations. To capture exploitation, which we define as the efficient gain of information along a reasoning path, we propose two novel derivatives of ER. Effective Rank Velocity (ERV), the first-order change, measures the velocity of this information gain, while Effective Rank Acceleration (ERA), the second-order change, captures the trend of velocity, indicating whether reasoning is accelerating or saturating. Equipped with these tools, we uncover a striking result: at the hidden-state level, exploration and exploitation show near-zero correlation (Fig. 1b, bottom). This contrast provides strong evidence that the trade-off is not an inherent property of RLVR for reasoning but an artifact of biased token-level measurements. It reveals that these two capacities are not antagonistic but can, in fact, *be decoupled and enhanced simultaneously* (Fig. 1c). Furthermore, by grouping questions based on correctness score, Fig. 2 demonstrates that the relationship between exploration and exploitation exhibits a consistent pattern, regardless of the modeling granularity (e.g., token-level vs. hidden states level). This result underscores the effectiveness of our proposed method for modeling exploration and exploitation.

Building on this core insight, we propose Velocity-Exploiting Rank-Learning (VERL), a method that moves beyond the trade-off between the two capacities by directly shaping the RL advantage function using ER and ERV. Instead of acting as a switch between the two capacities in lower dimension, VERL functions as a *tuner* synergistically enhances both capacities in higher dimension. Its key innovation is leveraging ERA as a meta-control variable, a choice justified by our theoretical proof of its remarkable $\mathcal{O}(1)$ growth stability (Sec. 3). Specifically, VERL uses ERA as a dynamic signal to enhance the training incentives; Specifically, VERL uses ERA to create a synergistic, dual-channel incentive structure. Instead of switching between modes, it prospectively shapes the reward to simultaneously encourage exploration (via ER) to preempt overconfidence, while also reinforcing exploitative gains (via ERV) to consolidate the reasoning path. This unique stability makes ERA a robust signal to guide training, allowing VERL to simultaneously encourage exploration from

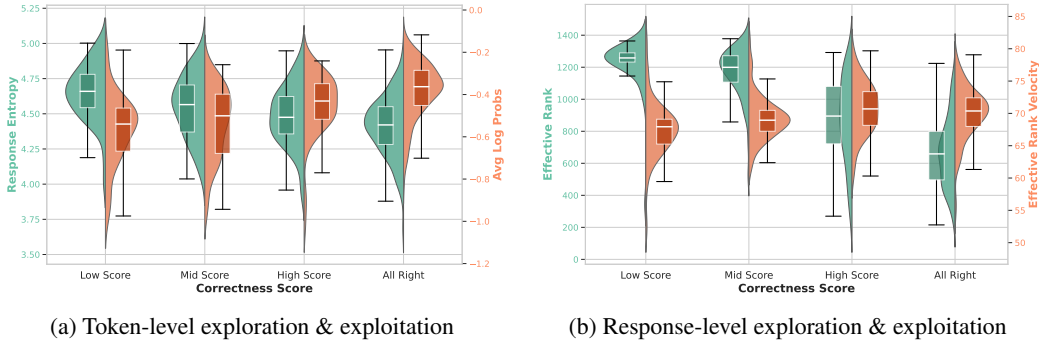


Figure 2: We conduct a comparative analysis against DeepSeek-R1-Distill-Qwen-7B on the simpleRL test dataset (Zeng et al., 2025), generating four distinct responses for each question via 4 separate rollouts. In (a) and (b), the horizontal axis represents the average correctness, quantifying the model’s mastery of the question. Notably, both the conventional token-level (a) and our proposed response-level (b) methods for modeling exploration and exploitation exhibit a consistent trend.

productive-potential states while preventing overfitting to local optima. As a result, VERL delivers significant performance gains across diverse models and tasks, achieving up to a **21.4%** absolute accuracy improvement on the challenging Gaokao 2024 benchmark.

Contributions. (i) We are the first to probe the exploration-exploitation relationship in the semantically rich hidden-state space. By adopting “ER” to quantify exploration and proposing novel metrics “ERV” and “ERA” for exploitation, we empirically demonstrate that these two capacities are decoupled, moving beyond the conventional token-level trade-off. (ii) We present VERL, a method that leverages ERA to manage exploration and exploitation in a unified framework, enabling the simultaneous enhancement of both capabilities. (iii) Our extensive experiments demonstrate the efficiency, generality, and versatility of VERL across different RL architectures.

2 PRELIMINARIES

2.1 PROBLEM FORMULATION AND NOTATIONS

We frame the training of LLMs for reasoning tasks as an RL problem. The LLM is modeled as a policy $\pi_\theta(\cdot|x)$, parameterized by θ , which generates a reasoning trajectory for a given prompt x sampled from a distribution \mathcal{P}_x . The model’s output is a sequence of reasoning steps $y_{0:T} = (y_0, y_1, \dots, y_T)$, constrained to a maximum length L_{\max} (i.e., $T < L_{\max}$). The quality of this trajectory is evaluated by a scalar reward function $r(x, y)$. The objective is to find the optimal policy π_ϕ that maximizes the expected reward:

$$\phi = \operatorname{argmax}_\theta \mathbb{E}_{x \sim \mathcal{P}_x} \mathbb{E}_{y \sim \pi_\theta(\cdot|x)} [r(x, y)] \text{ s.t. } |y| \leq L_{\max}. \tag{1}$$

Conventionally, optimizing this objective at the token level is framed as a fundamental exploration-exploitation trade-off. The policy must explore diverse and potentially novel reasoning pathways to discover high-reward solutions. Concurrently, it must exploit known strategies by reinforcing correct and reliable reasoning patterns that consistently yield high rewards.

2.2 REINFORCEMENT LEARNING BASELINE FRAMEWORKS

Proximal Policy Optimization (PPO) from Schulman et al. (2017) is a standard RL algorithm that seeks to maximize a clipped surrogate objective function. This objective prevents excessively large changes that would destabilize training, which is defined as:

$$\mathcal{L}_{\text{PPO}}(\theta) := \mathbb{E}_{x \sim \mathcal{P}_x, y \sim \pi_{\theta_{\text{old}}}(y|x)} \left\{ \sum_{t=1}^{|y|} \min [\rho_t(\theta) A_t, \text{clip}(\rho_t(\theta), 1 - \epsilon_{\text{low}}, 1 + \epsilon_{\text{high}}) A_t] \right\}, \tag{2}$$

where $\rho_t(\theta) := \frac{\pi_\theta(y_t|x, y_{<t})}{\pi_{\theta_{\text{old}}}(y_t|x, y_{<t})}$ is the probability ratio between the current and old policies, and A_t is the estimated advantage, often calculated using Generalized Advantage Estimation (GAE) from Schulman et al. (2015), with clipping (hyperparameter ϵ) to mitigate excessive deviation.

Group Relative Policy Optimization (GRPO) from [Shao et al. \(2024\)](#) computes a baseline directly from the rewards of multiple trajectories. For a given prompt, it samples a group of G responses, obtains their corresponding rewards $\{r_1, \dots, r_G\}$, and normalizes these rewards to compute the advantage for each response:

$$A_{i,t} := \frac{r_i - \text{mean}(\{r_j\}_{j=1}^G)}{\text{std}(\{r_j\}_{j=1}^G)}. \quad (3)$$

GRPO would assign a single rule-based reward to the entire output sequence, and the resulting group-relative advantage is uniformly propagated to all tokens, then updated as in Eq. 2.

2.3 CHARACTERIZING HIDDEN STATE REPRESENTATIONS

Response Hidden States. LLM would generate responses token by token in an autoregressive manner. The token y_t output at step t represents the current explicit state, while the corresponding output in the intermediate layers is referred to as the hidden state z_t . As the sequence of explicit states forms the final response, simultaneously, the hidden states $\{z_t\}_{t=1}^T$, ordered by their output sequence, collectively form the hidden states matrix $\mathbf{Z} \in \mathbb{R}^{T \times D}$, where T is the output length and D is the feature dimension, representing the semantic trajectory. To align with the semantic space, we focus on the hidden state of the final layer in this paper.

Dataset Hidden States. Following the definition in [Skean et al. \(2025\)](#), for a dataset containing N prompts, after obtaining a single vector representation for the i -th response by averaging its token hidden states $\bar{z}_i = \frac{1}{T_i} \sum_{t=1}^{T_i} z_{i,t}$, we stack these N mean embeddings in the dataset hidden states matrix $\bar{\mathbf{Z}} \in \mathbb{R}^{N \times D}$, to represent the overall semantic distribution of the entire dataset.

3 A HIDDEN-STATE PERSPECTIVE ON REPRESENTATIONAL DYNAMICS

3.1 STATIC METRIC: EFFECTIVE RANK (ER)

According to [Roy & Vetterli \(2007\)](#), the Effective Rank (ER), which is denoted by $\text{erank}(\mathbf{Z})$ for a response, is computed based on the normalized singular values of its non-padding hidden states \mathbf{Z} . Let σ_j be the j -th singular value of \mathbf{Z} , and $p_j = \frac{\sigma_j}{\sum_k \sigma_k}$ be the normalized singular values. The ER is then given by:

$$\text{ER} := \text{erank}(\mathbf{Z}) = \exp \left[- \sum_j p_j \log(p_j) \right]. \quad (4)$$

To quantify a model’s reasoning breadth, we treat exploration as a measurable semantic property. Our primary metric for this is ER, which measures the **effective dimensionality** of the hidden-state space a model occupies during a response. A high ER signals that the model is leveraging a rich and diverse set of internal features, which is a direct signature of exploratory behavior. A low ER, in contrast, points to a collapsed, simpler representation, indicating the model is not exploring widely. By capturing this dispersion of embeddings, ER provides a more nuanced view of exploration than conventional rank, which merely counts dimensions without considering their diversity.

Theorem 3.1. *Suppose we have a matrix of embeddings $\mathbf{Z} \in \mathbb{R}^{T \times D}$. Then the ER of \mathbf{Z} is a lower bound of conventional rank of \mathbf{Z} :*

$$1 \leq \text{erank}(\mathbf{Z}) \leq \text{rank}(\mathbf{Z}) \leq \min\{T, D\}. \quad (5)$$

Remark 3.2. Conventional rank offers a discrete count of available dimensions but fails to capture the geometric complexity essential for true exploration. In contrast, ER provides a nuanced, continuous measure of “effective dimensionality”. In reasoning, this distinction is critical: conventional rank may count many potential paths, but ER reveals how uniformly the model is actually exploring them. A high ER reflects a more uniform distribution, signaling a broader and more effective exploration of the solution space.

3.2 DYNAMIC METRICS: EFFECTIVE RANK VELOCITY (ERV) AND ACCELERATION (ERA)

In this section, we develop temporal higher-order metrics, termed ERV and ERA, to characterize the dynamics of a policy’s information gain together. Corresponding to the first and second-order temporal differences of a representational metric, these tools measure how the quality of hidden states evolves, revealing whether the reasoning process is expanding, stabilizing, or saturating.

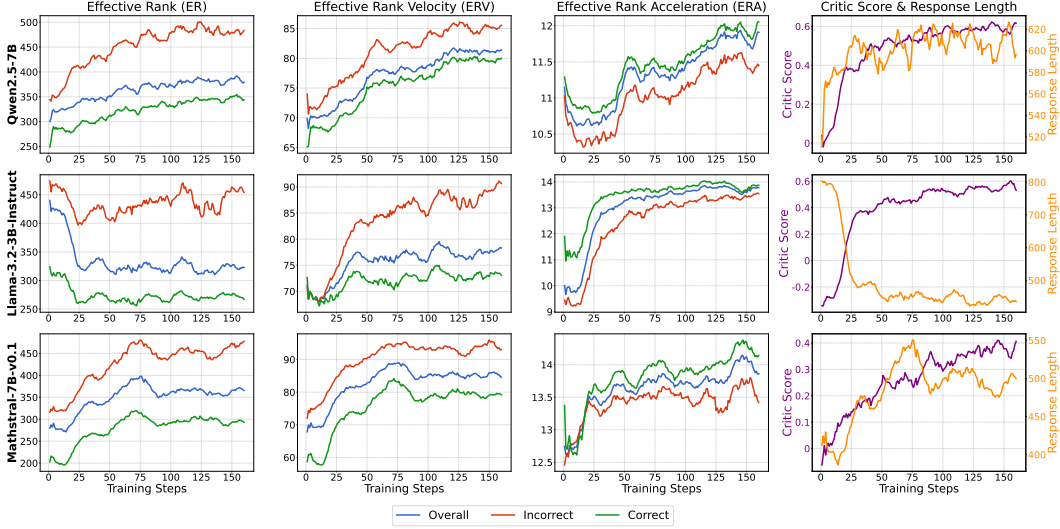


Figure 3: Response-level metrics during GRPO post-training, smoothed with a 10-step rolling window. Metrics are shown for the Overall batch, as well as for subsets of Correct and Incorrect samples. The rightmost column displays the average Critic Score (reward) and Response Length per batch.

Definition 3.3. (First-Order Temporal Difference: ERV) To quantify the rate of change for a given metric M , such as the ER or conventional rank of the hidden states matrix, we define the first-order temporal difference, denoted $\Delta_M^{(1)}$. This metric captures the “velocity” of information gain by measuring how the metric’s value at a given step deviates from its historical average. Let m_t be the value of metric M computed on the token sub-sequence from the start to position t . For a sequence of length T and a difference stride s , let the set of evaluation time steps be $\mathcal{T} = \{s, 2s, \dots, Ks\}$, where $K = \lfloor (T-1)/s \rfloor$. The overall first-order difference is defined as:

$$\Delta_M^{(1)} := \frac{1}{K-1} \sum_{j=2}^K \delta_{j \cdot s}, \quad \text{where} \quad \delta_{j \cdot s} := m_{j \cdot s} - \frac{1}{j-1} \sum_{k=1}^{j-1} m_{k \cdot s}. \quad (6)$$

Our primary metric for exploitation is ERV, which is designed to capture the rate of information gain. It is the average of instantaneous differences ($\delta_{j \cdot s}$), where each difference contrasts the complexity of the current token chunk with the cumulative average of all preceding ones. This formulation directly operationalizes our definition of exploitation: a large ERV demonstrates that the model is successfully enriching its representation at a rate that outpaces its historical trend, signifying a deepening and productive line of inquiry. Conversely, a small ERV signals that exploitation of the current path is becoming less effective.

Definition 3.4. (Second-Order Temporal Difference: ERA) To measure the rate of change of the velocity, we define the second-order temporal difference $\Delta_M^{(2)}$, which represents the “acceleration” of the metric’s evolution. It reveals whether the process of representation formation is speeding up or stabilizing. It is computed as the average change between consecutive instantaneous differences:

$$\Delta_M^{(2)} := \frac{1}{K-2} \sum_{j=3}^K [\delta_{j \cdot s} - \delta_{(j-1) \cdot s}]. \quad (7)$$

A positive $\Delta_M^{(2)}$ signifies an accelerating growth rate, indicating that the diversification of the representation is speeding up. A negative value suggests this growth is decelerating, implying that the representation’s quality is approaching stability or saturation.

3.3 SCALING PROPERTIES OF REPRESENTATIONAL DYNAMICS

In the preceding sections (Sec. 3.1 and 3.2), we introduced metrics for analyzing the hidden states of individual responses. We now analyze the scaling properties of these dynamics at two distinct levels of granularity: across an entire dataset as a function of its size (N), and within a single reasoning

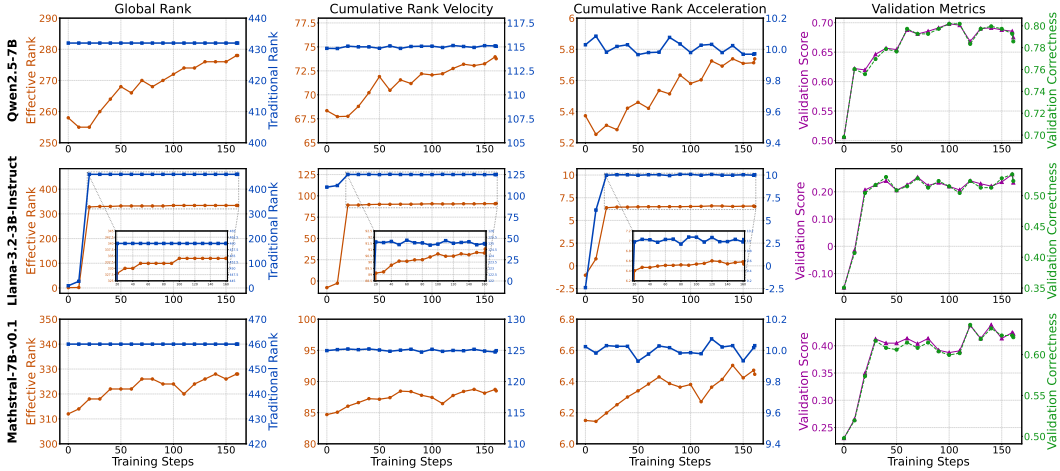


Figure 4: Visualization of dataset-level metrics during GRPO post-training. The figure compares Traditional metrics with our proposed metrics. Also shown are the Validation Score and sample Correctness, both averaged over the validation dataset.

trajectory as a function of its length (T). The following proposition provides a unified theoretical model for both scenarios.

Proposition 3.5. Assume a hidden-state matrix is composed of k approximately orthogonal row vectors. The Effective Rank (ER) and its first-order difference (ERV) scale linearly with k , such that $ER = \mathcal{O}(k)$ and $\Delta_{ER}^{(1)} = \mathcal{O}(k)$. The second-order difference (ERA) is independent of k , with a scaling order of $\Delta_{ER}^{(2)} = \mathcal{O}(1)$.

Remark 3.6. This proposition offers a dual interpretation of how our metrics scale under ideal conditions: **At the dataset level**, k represents the number of questions N . The proposition implies that as a dataset grows with semantically distinct responses (approaching orthogonality), its overall representational diversity (ER) should increase proportionally. The constant acceleration (ERA) suggests a stable, predictable growth pattern for the dataset’s semantic volume. **At the response level**, k represents the sequence length T . The proposition suggests that for an ideal reasoning process where each step contributes novel information (making token embeddings approach orthogonality), the trajectory’s semantic complexity (ER) and information-gain velocity (ERV) should also grow linearly with its length. In this context, a constant ERA becomes a signature of a robust and non-saturating reasoning process.

4 DECOUPLING EXPLORATION AND EXPLOITATION IN REASONING

In this section, we first investigate the changing trends of the hidden states matrix rank (both ER and conventional rank) during regular RL training. Specifically, we utilized the Qwen (Hui et al., 2024) and Llama (Dubey et al., 2024) models for our experiments, employing GRPO (Shao et al., 2024) reinforcement learning paradigm. The training dataset followed the configuration in Zeng et al. (2025), which comprises 8k hard-level 3 to 5 mathematical problems from MATH datasets, each accompanied by a verifiable reference answer.

4.1 ANALYSIS OF RESPONSE-LEVEL METRICS

During each training step, we quantitatively analyzed the representational dynamics of hidden states within that batch as depicted in Fig. 3, and provided more and diverse details in App. E.1.

Semantic space of hidden states move beyond the exploration-exploitation trade-off towards stable enhancements. While RL consistently improves performance, it interacts differently with distinct base models, evidenced in the divergent trends of the ER (first column in Fig. 3), which measures the total information within a response. For instance, the Qwen model exhibits an increasing ER, suggesting more exploratory reasoning, whereas the one of Llama model decreases, indicating more concise, exploitative reasoning. Despite these differences in exploratory behavior, the ERV (second column) demonstrates a consistent upward scaling trend for all models, which sug-

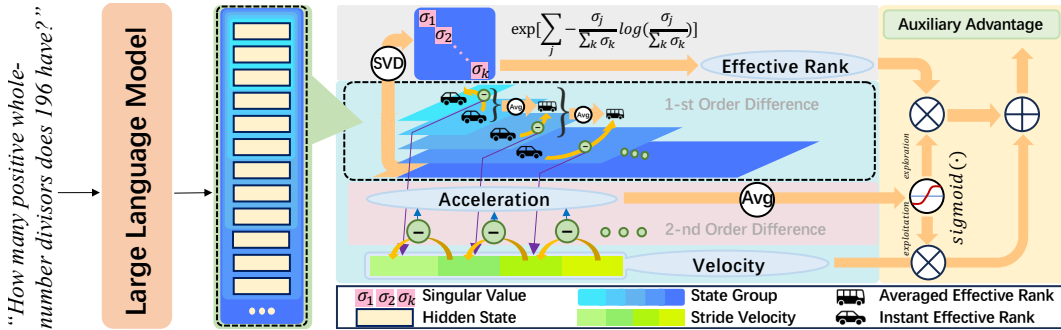


Figure 5: Overview of VERL. Exploration is quantified by computing the ER of the rolling-done hidden states via SVD, while exploitation is captured through EMA-smoothed first-order difference (ERV) on per-step rolling hidden state and extended to second-order difference (ERA). Finally, exploration and exploitation are adaptively integrated to derive the auxiliary advantage.

gests while the models’ intrinsic exploratory tendencies differ, RL fine-tuning universally enhances their exploitation capabilities by consistently accelerating the rate of information gain.

ERA distinguishes correct reasoning. For both the zero-order metric (ER) and the first-order metric (ERV), incorrect reasoning paths consistently score higher than correct ones. This suggests that excessive exploration (high ER) with new excessive information (high ERV) will potentially derail the reasoning process and lead to incorrect answers. Conversely, for the second-order metric (ERA), correct reasoning trajectories consistently exhibit higher values, which implies the acceleration of information gain—the ability to increasingly speed up the representational evolution—is the key to guide the policy towards a correct solution, distinguishing robust reasoning from flawed exploration.

4.2 ANALYSIS OF DATASET-LEVEL METRICS

Following the framework established in Sec. 2, we extend our analysis from the response level to the entire validation dataset. By computing the dataset hidden states matrix $\bar{\mathbf{Z}}$, we examine its zero-, first-, and second-order rank dynamics to understand how the policy’s overall representational space evolves. The trends are visualized in Fig. 4. While key experiments are shown here, we refer the reader to App. E.2 for a more diverse range of studies.

Policy optimization correlates with expanding dataset-level diversity. Across the training process, we observe a strong positive correlation between performance metrics (accuracy and critic score on the validation set) and the dynamics of dataset-level ER. As the model improves, the zero-order $\text{erank}(\bar{\mathbf{Z}})$ and its first- and second-order differences consistently scale up. This indicates that as the policy is updated, it develops a more diverse and complex repertoire of reasoning strategies for the same set of problems. The increasing ERV and ERA suggest the model becomes progressively more efficient at navigating and expanding this richer semantic space to discover correct solutions.

ER reveals refinement beyond the limits of conventional rank. During late-stage training, a plateauing conventional rank suggests the model has settled on a fixed number of linearly independent reasoning “directions”. Yet, a simultaneously rising ER points to a more subtle optimization. This trend reveals that the model is improving the quality of its existing solution space by making the “magnitudes” of these directions more uniform. In essence, instead of finding new pathways, the model learns to utilize its established ones more equitably, reducing representational redundancy and fostering a more sophisticated and distributed reasoning capability.

5 VELOCITY-EXPLOITING RANK-LEARNING (VERL)

Building upon the insights from Sec. 3 and the empirical observations in Sec. 4, we find that conventional RL objectives overlook the intrinsic hidden-state dynamics that more faithfully characterize exploration and exploitation. This oversight may lead to inefficient training, where policies either wander in unproductive exploration or collapse prematurely to suboptimal reasoning paths. To address this, we propose a novel method named Velocity-Exploiting Rank-Learning (VERL), which refines advantage by incorporating the nuanced dynamics of hidden states, enabling simultaneous enhancement of exploration and exploitation capacities.

5.1 STABLE REPRESENTATION DEVIATION INDICATOR

Concretely, we first formalize the representational metrics, letting $\mathcal{M} = \{M_0, M_1, M_2\}$ denote the set of metrics derived from the hidden states, where M_0 is the 0-order ER, $M_1 := \Delta_M^{(1)}$ is its first-order temporal difference (ERV), and $M_2 := \Delta_M^{(2)}$ is its second-order temporal difference (ERA). To create a stable guidance signal, having already computed scalar values $\{m_0, m_1, m_2\}$ for each trajectory, we normalize these values against their historical trends by maintaining an Exponential Moving Average (EMA) $\bar{\mu}_k$ for each metric M_k . The relative deviation for each metric is:

$$d_k := \frac{m_k - \bar{\mu}_k}{|\bar{\mu}_k| + \epsilon}, \quad k \in \{0, 1, 2\}, \quad (8)$$

where ϵ is a small constant for numerical stability. This deviation d_k quantifies how the current trajectory’s representational structure diverges from the policy’s recent average behavior.

5.2 BEYOND TRADE-OFF FOR EFFICIENT TRAINING VIA ERA

Our analysis in Sec. 3.1 and 3.2 reveals that ER (M_0) and ERV (M_1) are effective proxies for exploration and exploitation, respectively. Crucially, these two metrics are also almost independent of each other, as shown in Fig. 1c bottom. This decoupling is key, as it allows us to combine them into a single objective to enhance both capabilities simultaneously. M_1 measures the confidence of the current step as analysis above, so the subtraction of M_1 , namely ERA (M_2), would predict the evolution of confidence in subsequent steps. Meanwhile, theoretical analysis (Prop. 3.5) and empirical observations (Fig. 4) indicate that M_2 remains approximately constant across trajectories. Thus, M_2 can serve as a meta-level signal to guide training.

An increasing ERV indicates that the model is acquiring progressively more informative evidence, reflecting its growing confidence. However, our preliminary experiments reveal that trajectories exhibiting excessively high confidence often achieve high in-domain performance (as evidenced by the results on the MATH dataset in Tab. 1, where performance suffers without ERA’s dynamic unification or when using a simple 50/50 sum “ $\beta = 0.5$.”) while compromising out-of-domain generalization (across most datasets), suggesting severe overfitting. This implies that overconfident trajectories reduce the opportunity to learn from less confident yet potentially informative samples. To mitigate this, we employ M_2 as the predictive signal to combine exploration and exploitation, strategically encouraging exploring lower-confidence samples when trajectories exhibit excessively high future confidence, thereby enhancing training efficiency and robustness.

Specifically, we define two orthogonal unit vectors of the weights first, an exploration-focused vector $\mathbf{w}_{\text{explore}} = [1, 0]$, which targets M_0 , and an exploitation-focused one $\mathbf{w}_{\text{exploit}} = [0, 1]$ of M_1 . The dynamic weight \mathbf{w}_{dyn} is interpolated by the relative deviation of the second-order metric d_2 :

$$\mathbf{w}_{\text{dyn}} := \beta \cdot \mathbf{w}_{\text{explore}} + (1 - \beta) \cdot \mathbf{w}_{\text{exploit}}, \quad \text{where } \beta := \text{sigmoid}(d_2). \quad (9)$$

The interpolation coefficient β is adaptively determined by the second-order metric d_2 through a sigmoid mapping. A high M_2 ($d_2 \gg 0$) means overconfidence in the future, risking overfitting to in-domain patterns; thus, VERL increases β to favor the exploration profile M_0 . In contrast, when M_2 is low ($d_2 \leq 0$), namely limited confidence and reasoning saturation, VERL decreases β to emphasize the exploitation profile M_1 . As M_2 typically fluctuates around zero, VERL jointly enhances exploration and exploitation. The final auxiliary advantage Φ is defined as:

$$\Phi := w_{\text{dyn},0} \cdot \tanh(d_0) + w_{\text{dyn},1} \cdot \tanh(d_1), \quad (10)$$

where $w_{\text{dyn},0}$ and $w_{\text{dyn},1}$ are the first and second entries of the dynamic weight vector \mathbf{w}_{dyn} , respectively. The tanh function bounds the magnitude of Φ while preserving its sign, thereby stabilizing training. This formulation rewards trajectories that exceed the historical average and penalizes those that fall short, guiding the policy with adaptive reasoning dynamics while mitigating risks of stagnation and overconfidence.

5.3 ADVANTAGE SHAPING VIA REPRESENTATIONAL DYNAMICS

Our core idea is to refine the learning signal by injecting an auxiliary term directly into the advantage function (termed as Advantage Shaping). Let $A^{(0)}$ be an original advantage estimate from a policy gradient algorithm (e.g., GRPO or PPO with GAE), and let Φ_i be the sequence-level auxiliary term

for trajectory i as defined in Sec. 5.2. We define the shaped advantage \hat{A} as follows:

$$\hat{A} := A^{(0)} + \min\left(\max(0, \Phi_i), \frac{|A^{(0)}|}{\kappa}\right), \quad (11)$$

where κ is a clipping factor for stable training. This shaping mechanism can apply seamlessly to different advantage structures. For GRPO, $A^{(0)}$ is the sequence-level advantage, and the shaping is applied once per trajectory. For PPO with GAE, $A^{(0)}$ is the per-token advantage estimation $A_t^{(0)}$, and the sequence-level term Φ_i is applied to each token’s advantage within that trajectory. In both cases, this reshaped advantage \hat{A} replaces the original estimation in the clipped surrogate objective function, directly influencing the gradient to guide policy optimization. More details in Algorithm 1.

Table 1: Pass@1 performance with variant β . “Adapted β ” denotes $\beta := \text{sigmoid}(d_2)$. In this paper, all results in the table are reported in percentage (%), with **Bold** indicating the best performance.

Training Strategy	Score Avg	In Domain			Out of Domain				Hard Problems				
		MATH	MATH500	Avg	Gaokao	CN Middle School	CMATH	Avg	AIME24	AIME25	AMC23	AMC24	Avg
GRPO	0.36	51.4	46.2	48.80	23.7	28.7	28.3	26.90	3.3	0.0	27.5	8.9	9.93
GRPO+VERL ($\beta = 0.5$)	0.38	51.2	47.2	49.20	21.2	36.6	38.7	32.17	10.0	0.0	27.5	8.9	11.60
GRPO+VERL (Adapted β)	0.38	50.9	51.2	51.05	22.9	38.6	46.2	35.90	13.3	6.7	20.0	11.1	12.78

6 EXPERIMENTS

6.1 EXPERIMENT SETTINGS

(i) **Dataset.** The same datasets as in Sec. 4 are used. (ii) **Reward.** Our rule-based reward function assesses mathematical correctness and `\boxed{\}` formatting. Correct answers receive a +1.0 reward if formatted, and +0.5 if not. Incorrect answers are penalized with -0.5 if formatted and -1.0 otherwise. (iii) **Training.** Based on verl (Sheng et al., 2025) and vLLM (Kwon et al., 2023) framework, we set batch size as 48, generating 4 rollouts per prompt for GRPO and 1 rollout for PPO, and set the maximum length L_{\max} to 1536. More details of the experiments are provided in App. D.

6.2 MAIN RESULTS

VERL Generalizes across Multiple Benchmarks of Varying Difficulty. As summarized in Tab. 2 (Full details in App. E.3), VERL leads to consistent performance gains across benchmarks of different difficulty levels, ranging from elementary school problems (e.g., ASDiv) to Olympiad-level challenges (e.g., OlympiadBench). The improvements are particularly pronounced on benchmarks that demand multi-step reasoning rather than simple arithmetic. VERL achieves up to 21.4% and 10.0% absolute accuracy improvements on Gaokao 2024_I and AIME24 (in Tab. 2), respectively.

VERL Generalizes across RL Algorithms and Base Models. VERL is a plug-and-play method that can be integrated with different RL algorithms to enhance their performance. As shown in Tab. 2, applying VERL to GRPO and PPO improves the average results on 15 benchmarks for both the Llama and Qwen series, demonstrating its strong generalization ability.

Gains in Both Exploration and Exploitation. As shown in Tab. 3 (Full details in App. E.4), VERL yields larger improvements on Pass@ k (a measure of exploration) than on Pass@1 (a measure of exploitation), particularly on more challenging benchmarks. Since Pass@1 reflects exploitation and Pass@ k reflects exploration, the combined results of Tab. 2 and Tab. 3 demonstrate that VERL effectively enhances both abilities. For a detailed case study, see Sec. F.

6.3 ABLATION ANALYSES

We conduct ablation studies on VERL’s key hyperparameters: the stride length (s) for temporal dynamics, the advantage clipping factor (κ), and the composition of the auxiliary shaping signal.

Analysis of Stride (s). The stride s determines the granularity for calculating temporal difference metrics. As depicted in Fig. 6 (a), VERL’s performance improvement is robust across various stride values, indicating the underlying signal is not overly sensitive to sampling frequency. We find that $s = 40$ yields optimal validation rewards, striking an effective balance between capturing significant temporal shifts and avoiding noise from minor token-level fluctuations.

Analysis of Advantage Clip (κ). The advantage clipping factor κ stabilizes training by ensuring our auxiliary term acts as a refinement rather than a dominant signal. It constrains the shaping bonus

Table 2: Performance comparison of models on mathematical reasoning benchmarks (Pass@1). “+ GRPO” and “+ PPO” denote RL fine-tuning by GRPO and PPO framework respectively. “w/ VERL.” indicates incorporating our VERL with original RL type. Δ represents the performance contrast between original RL method and its VERL variant. See App. E.3 for full details.

Model	AIME24	AIME25	AMC23	AMC24	ASDiv	Carp.En	CMATH	Gaokao 2024.1	Gaokao 2024.Mix	Gaokao MathCloze	GSM8K	MAWPS	Olympiad Bench	SVAMP	TabMWP	Avg.
Llama-3.2-3B-Instruct	0.0	0.0	25.0	11.1	74.6	26.5	10.2	14.3	14.3	6.8	66.6	86.9	12.7	74.1	41.4	31.0
+ GRPO	3.3	0.0	27.5	8.9	88.8	45.0	28.3	21.4	20.9	23.7	80.7	96.0	16.7	87.7	71.7	41.4
+ GRPO w/ VERL.	13.3	6.7	25.0	11.1	89.3	45.4	46.2	14.3	22.0	22.9	81.7	96.0	17.6	87.8	72.3	43.4
Δ_{GRPO}	+10.0	+6.7	-2.5	+2.2	+0.5	+0.4	+17.9	-7.1	+1.1	-0.8	+1.5	+0.0	+0.9	+0.1	+0.6	+2.0
+ PPO	10.0	3.3	22.5	13.3	87.9	46.4	21.2	7.1	16.5	20.3	81.4	95.5	17.8	86.8	71.0	40.1
+ PPO w/ VERL.	10.0	3.3	25.0	11.1	88.7	46.0	30.7	14.3	19.8	27.1	82.9	95.7	17.3	85.8	71.3	41.9
Δ_{PPO}	+0.0	+0.0	+2.5	-2.2	+0.8	-0.4	+9.5	+7.2	+3.3	+6.8	+1.5	+0.2	-0.5	-1.0	+0.3	+1.9
Qwen2.5-7B	6.7	0.0	45.0	15.6	91.4	55.8	86.7	42.9	33.0	49.2	85.8	95.4	25.8	88.5	82.8	53.6
+ GRPO	10.0	6.7	55.0	26.7	94.8	60.2	91.7	14.3	34.1	64.4	90.2	97.6	36.1	92.8	91.3	57.7
+ GRPO w/ VERL.	13.3	10.0	50.0	28.9	95.0	60.8	90.7	35.7	35.2	69.5	89.2	97.7	35.4	92.9	91.9	59.8
Δ_{GRPO}	+3.3	+3.3	-5.0	+2.2	+0.2	+0.6	-1.0	+21.4	+1.1	+5.1	-1.0	+0.1	-0.7	+0.1	+0.6	+2.1
+ PPO	6.7	3.3	50.0	33.3	94.9	59.6	89.8	28.6	31.9	63.6	89.1	97.3	36.1	92.8	90.8	57.9
+ PPO w/ VERL.	10.0	6.7	52.5	33.3	94.8	60.0	90.3	28.6	34.1	66.9	90.2	97.8	36.1	92.5	90.6	59.0
Δ_{PPO}	+3.3	+3.3	+2.5	+0.0	-0.1	+0.4	+0.5	+0.0	+2.2	+3.3	+1.1	+0.5	+0.0	-0.3	-0.2	+1.1
Mathstral-7B-v0.1	0.0	0.0	12.5	8.9	87.1	51.1	74.2	28.6	33.0	31.4	81.6	93.8	17.9	87.7	54.7	44.2
+ GRPO	0.0	0.0	47.5	17.8	92.9	55.9	81.3	35.7	44.0	49.2	88.1	97.6	25.6	93.0	81.5	54.0
+ GRPO w/ VERL.	6.7	0.0	45.0	20.0	93.3	55.5	81.5	50.0	40.7	46.6	89.5	97.2	29.3	90.7	83.5	55.3
Δ_{GRPO}	+6.7	+0.0	-2.5	+2.2	+0.4	-0.4	+0.2	+14.3	+3.3	-2.6	+1.4	-0.4	+3.7	-2.3	+2.0	+1.3
+ PPO	6.7	3.3	32.5	20.0	90.9	51.8	78.3	42.9	37.4	49.2	87.0	96.0	28.4	89.9	70.7	52.3
+ PPO w/ VERL.	10.0	0.0	27.5	22.2	93.0	53.8	78.2	42.9	51.6	48.3	87.4	96.7	26.1	89.6	84.1	54.1
Δ_{PPO}	+3.3	-3.3	-5.0	+2.2	+2.1	+2.0	-0.1	+0.0	+14.2	-0.9	+0.4	+0.7	-2.3	-0.3	+13.4	+1.8

Table 3: Performance comparison of instruction-tuned models under diverse decoding settings (Pass@k). For full details, please refer to App. E.4.

Model	MATH500 (Pass@16)	AMC23 (Pass@128)	AMC24 (Pass@128)	AIME24 (Pass@256)	AIME25 (Pass@256)	Avg.
Llama-3.2-3B-Instruct	79.8	93.5	51.5	40.0	30.0	58.96
+ GRPO	80.2	95.4	60.6	40.0	30.0	61.24
+ GRPO w/ VERL.	80.6	95.7	59.0	50.0	36.7	64.40
Δ_{GRPO}	+0.4	+0.3	-1.6	+10.0	+6.7	+3.16
+ PPO	82.2	94.5	57.0	46.7	36.7	63.42
+ PPO w/ VERL.	82.4	94.7	57.8	46.7	40.0	64.32
Δ_{PPO}	+0.2	+0.2	+0.8	+0.0	+3.3	+0.90
Qwen2.5-7B	90.6	98.4	73.7	60.0	60.0	76.54
+ GRPO	90.8	97.8	78.3	56.7	50.0	74.72
+ GRPO w/ VERL.	91.4	98.3	79.0	63.3	60.0	78.40
Δ_{GRPO}	+0.6	+0.5	+0.7	+6.6	+10.0	+3.68
+ PPO	91.2	98.6	74.3	53.3	56.7	74.82
+ PPO w/ VERL.	91.4	98.0	74.4	56.7	66.7	77.44
Δ_{PPO}	+0.2	-0.6	+0.1	+3.4	+10.0	+2.62
Mathstral-7B-v0.1	80.4	88.5	60.9	43.3	36.7	61.96
+ GRPO	84.8	87.3	69.2	36.7	40.0	63.60
+ GRPO w/ VERL.	87.0	97.0	76.9	50.0	50.0	72.18
Δ_{GRPO}	+2.2	+9.7	+7.7	+13.3	+10.0	+8.58
+ PPO	82.4	91.7	70.7	53.3	40.0	67.62
+ PPO w/ VERL.	84.8	93.8	69.9	53.3	46.7	69.70
Δ_{PPO}	+2.4	+2.1	-0.8	+0.0	+6.7	+2.08

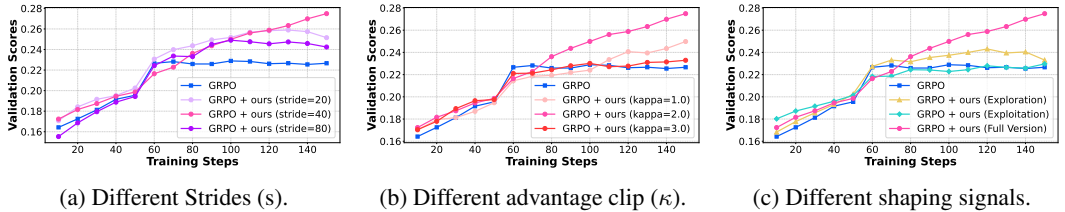


Figure 6: Comparison of various hyperparameters with Llama-3.2-3B-Instruct.

to a fraction of the original advantage, preventing it from overpowering the primary task reward. The results in Fig. 6 (right) show that VERL consistently enhances performance for all tested values of κ underscoring its stability. Optimal performance is achieved at $\kappa = 2$, which provides a sufficiently strong and well-proportioned signal to guide the policy without destabilizing the learning process.

Analysis of Shaping Signals (Φ). Compared to the full formulation in Eq. 10, using only the exploration-related term prevents the model from exploiting high-reward trajectories, leading to earlier bottlenecks and inferior final performance. In contrast, using only the exploitation-related term yields higher initial returns but quickly plateaus due to insufficient exploration. When combining both terms, the model achieves more stable training and superior final performance.

7 RELATED WORK

Reinforcement Learning with Verifiable Rewards. To unlock the full reasoning potential of Large Language Models (LLMs), Reinforcement Learning with Verifiable Rewards (RLVR) has become a prominent training paradigm. This approach was notably employed by DeepSeek-R1-Zero (Guo et al., 2025) and , which executes complex reasoning processes through actions such as

reflection and validation. Following the success of DeepSeek-R1, a significant body of research has investigated the efficacy of RLVR on popular open-source LLMs, including Qwen (Yang et al., 2024), Mistral (Jiang et al., 2024), and LLaMA (Dubey et al., 2024).

This has fostered an optimistic view that RLVR can not only enhance existing model capabilities but also enable the acquisition of novel reasoning knowledge, facilitating a path toward continuous self-improvement (Zeng et al., 2025; Yu et al., 2025). RLVR training has been shown to grant LLMs controllable output length for efficient inference (Yan et al., 2025; Cheng et al., 2025b), deepen their reasoning pathways (Bensal et al., 2025), mitigate their weaknesses (Liang et al., 2025a;b), enable the use of external tools (Rainone et al., 2025; Jin et al., 2025), and even facilitate unsupervised reasoning (Zuo et al., 2025). However, some studies (Yue et al., 2025) argue that while RLVR significantly improves the confidence and reliability of model reasoning, it may inadvertently constrain the model’s exploratory capacity. The core of this issue lies in RLVR’s optimization objective: maximizing expected rewards. This objective function inherently biases the policy gradient toward reinforcing known trajectories that lead to high rewards (i.e., “exploitation”), while suppressing the exploration of unknown paths that may offer potentially higher returns but also carry greater risk (i.e., “exploration”). Consequently, the outputs of RLVR-optimized models often remain confined within the sampling distribution of the base model, suggesting the paradigm excels at refining existing knowledge rather than generating new knowledge. This trade-off between exploration and exploitation constitutes a central challenge in the contemporary RLVR landscape.

Exploration and Exploitation in Reinforcement Learning. Recent perspectives (Wang et al., 2025; Cui et al., 2025) on the exploration-exploitation dilemma have predominantly been shaped by analyses at the token level, focusing on the prediction distribution over the vocabulary. From this viewpoint, higher entropy in the token-level prediction—indicating a more uniform distribution over the next token—is interpreted as a sign of greater exploratory behavior, as it suggests a capacity for more diverse responses. This has led to the adoption of techniques (Deng et al., 2025; Cheng et al., 2025a) such as entropy regularization to explicitly encourage the policy to explore novel reasoning paths. Conversely, lower entropy in the token-level prediction is taken to signify higher model confidence in its reasoning chain, thus representing strong exploitation. Subsequent work (Fu et al., 2025) has also utilized metrics derived from the top-k probabilities of the token prediction to quantify confidence. For instance, some approaches (Damani et al., 2025; Qiao et al., 2025) leverage the model’s internal “confidence” signals to dynamically evaluate and filter the quality of reasoning steps, while others have employed high confidence as a feedback signal to enable unsupervised reinforcement learning (Li et al., 2025b). Ultimately, however, these confidence-based metrics are not fundamentally different from entropy. This token-level standard of measurement introduces an endogenous contradiction: classifying behavior as either exploratory or exploitative requires the introduction of a prior assumption, a practice that is disadvantageous for LLM research.

In this paper, we depart from this paradigm. We shift the analysis from the token level to the semantic space at the response level. This approach allows us to decouple the intertwined elements of exploration and exploitation, aiming to achieve a simultaneous enhancement of both during reinforcement learning.

8 CONCLUSION

We challenge the conventional exploration-exploitation capacities trade-off in LLM reasoning blamed on token-level analysis and shift focus to their decoupled relation in hidden-state representations (measured as semantic diversity and information gain velocity, respectively). We introduce ER, ERV and ERA to quantify the dynamics of semantic complexity, with ERA as a stable indicator distinguishing correct from flawed reasoning. We further propose Velocity-Exploiting Rank-Learning (VERL) method, which uses ERA as a meta-controller to adaptively shape the advantage function, moving beyond the trade-off for simultaneous enhancement. Extensive experiments validate VERL’s superior out-of-domain generalization and performance on complex reasoning tasks.

REFERENCES

- Shivam Agarwal, Zimin Zhang, Lifan Yuan, Jiawei Han, and Hao Peng. The unreasonable effectiveness of entropy minimization in llm reasoning. *arXiv preprint arXiv:2505.15134*, 2025.
- Shelly Bensal, Umar Jamil, Christopher Bryant, Melisa Russak, Kiran Kamble, Dmytro Mozolevskyi, Muayad Ali, and Waseem AlShikh. Reflect, retry, reward: Self-improving llms via

- reinforcement learning. *arXiv preprint arXiv:2505.24726*, 2025.
- Shuang Chen, Yue Guo, Zhaochen Su, Yafu Li, Yulun Wu, Jiacheng Chen, Jiayu Chen, Weijie Wang, Xiaoye Qu, and Yu Cheng. Advancing multimodal reasoning: From optimized cold start to staged reinforcement learning. *arXiv preprint arXiv:2506.04207*, 2025a.
- Zhipeng Chen, Xiaobo Qin, Youbin Wu, Yue Ling, Qinghao Ye, Wayne Xin Zhao, and Guang Shi. Pass@ k training for adaptively balancing exploration and exploitation of large reasoning models. *arXiv preprint arXiv:2508.10751*, 2025b.
- Daixuan Cheng, Shaohan Huang, Xuekai Zhu, Bo Dai, Wayne Xin Zhao, Zhenliang Zhang, and Furu Wei. Reasoning with exploration: An entropy perspective. *arXiv preprint arXiv:2506.14758*, 2025a.
- Zhengxiang Cheng, Dongping Chen, Mingyang Fu, and Tianyi Zhou. Optimizing length compression in large reasoning models. *arXiv preprint arXiv:2506.14755*, 2025b.
- Karl Cobbe, Vineet Kosaraju, Mohammad Bavarian, Mark Chen, Heewoo Jun, Lukasz Kaiser, Matthias Plappert, Jerry Tworek, Jacob Hilton, Reiichiro Nakano, et al. Training verifiers to solve math word problems. *arXiv preprint arXiv:2110.14168*, 2021.
- Ganqu Cui, Yuchen Zhang, Jiacheng Chen, Lifan Yuan, Zhi Wang, Yuxin Zuo, Haozhan Li, Yuchen Fan, Huayu Chen, Weize Chen, et al. The entropy mechanism of reinforcement learning for reasoning language models. *arXiv preprint arXiv:2505.22617*, 2025.
- Mehul Damani, Isha Puri, Stewart Slocum, Idan Shenfeld, Leshem Choshen, Yoon Kim, and Jacob Andreas. Beyond binary rewards: Training llms to reason about their uncertainty. *arXiv preprint arXiv:2507.16806*, 2025.
- Jia Deng, Jie Chen, Zhipeng Chen, Daixuan Cheng, Fei Bai, Beichen Zhang, Yinqian Min, Yanzipeng Gao, Wayne Xin Zhao, and Ji-Rong Wen. From trial-and-error to improvement: A systematic analysis of llm exploration mechanisms in rlvr. *arXiv preprint arXiv:2508.07534*, 2025.
- Abhimanyu Dubey, Abhinav Jauhri, Abhinav Pandey, Abhishek Kadian, Ahmad Al-Dahle, Aiesha Letman, Akhil Mathur, Alan Schelten, Amy Yang, Angela Fan, et al. The llama 3 herd of models. *arXiv e-prints*, pp. arXiv–2407, 2024.
- Yichao Fu, Xuwei Wang, Yuandong Tian, and Jiawei Zhao. Deep think with confidence. *arXiv preprint arXiv:2508.15260*, 2025.
- Daya Guo, Dejian Yang, Haowei Zhang, Junxiao Song, Ruoyu Zhang, Runxin Xu, Qihao Zhu, Shirong Ma, Peiyi Wang, Xiao Bi, et al. Deepseek-r1: Incentivizing reasoning capability in llms via reinforcement learning. *arXiv preprint arXiv:2501.12948*, 2025.
- Chaoqun He, Renjie Luo, Yuzhuo Bai, Shengding Hu, Zhen Thai, Junhao Shen, Jinyi Hu, Xu Han, Yujie Huang, Yuxiang Zhang, et al. Olympiadbench: A challenging benchmark for promoting agi with olympiad-level bilingual multimodal scientific problems. In *Proceedings of the 62nd Annual Meeting of the Association for Computational Linguistics (Volume 1: Long Papers)*, pp. 3828–3850, 2024.
- Dan Hendrycks, Collin Burns, Saurav Kadavath, Akul Arora, Steven Basart, Eric Tang, Dawn Song, and Jacob Steinhardt. Measuring mathematical problem solving with the math dataset. *arXiv preprint arXiv:2103.03874*, 2021.
- Binyuan Hui, Jian Yang, Zeyu Cui, Jiayi Yang, Dayiheng Liu, Lei Zhang, Tianyu Liu, Jiajun Zhang, Bowen Yu, Keming Lu, et al. Qwen2. 5-coder technical report. *arXiv preprint arXiv:2409.12186*, 2024.
- Albert Q Jiang, Alexandre Sablayrolles, Antoine Roux, Arthur Mensch, Blanche Savary, Chris Bamford, Devendra Singh Chaplot, Diego de las Casas, Emma Bou Hanna, Florian Bressand, et al. Mixtral of experts. *arXiv preprint arXiv:2401.04088*, 2024.

- Bowen Jin, Hansi Zeng, Zhenrui Yue, Jinsung Yoon, Sercan Arik, Dong Wang, Hamed Zamani, and Jiawei Han. Search-rl: Training llms to reason and leverage search engines with reinforcement learning. *arXiv preprint arXiv:2503.09516*, 2025.
- Rik Koncel-Kedziorski, Subhro Roy, Aida Amini, Nate Kushman, and Hannaneh Hajishirzi. Mawps: A math word problem repository. In *Proceedings of the 2016 conference of the north american chapter of the association for computational linguistics: human language technologies*, pp. 1152–1157, 2016.
- Woosuk Kwon, Zhuohan Li, Siyuan Zhuang, Ying Sheng, Lianmin Zheng, Cody Hao Yu, Joseph Gonzalez, Hao Zhang, and Ion Stoica. Efficient memory management for large language model serving with pagedattention. In *Proceedings of the 29th symposium on operating systems principles*, pp. 611–626, 2023.
- Junyan Li, Wenshuo Zhao, Yang Zhang, and Chuang Gan. Steering llm thinking with budget guidance. *arXiv preprint arXiv:2506.13752*, 2025a.
- Pengyi Li, Matvey Skripkin, Alexander Zubrey, Andrey Kuznetsov, and Ivan Oseledets. Confidence is all you need: Few-shot rl fine-tuning of language models. *arXiv preprint arXiv:2506.06395*, 2025b.
- Xiao Liang, Zhong-Zhi Li, Yeyun Gong, Yang Wang, Hengyuan Zhang, Yelong Shen, Ying Nian Wu, and Weizhu Chen. Sws: Self-aware weakness-driven problem synthesis in reinforcement learning for llm reasoning. *arXiv preprint arXiv:2506.08989*, 2025a.
- Xiao Liang, Zhongzhi Li, Yeyun Gong, Yelong Shen, Ying Nian Wu, Zhijiang Guo, and Weizhu Chen. Beyond pass@ 1: Self-play with variational problem synthesis sustains rlvr. *arXiv preprint arXiv:2508.14029*, 2025b.
- Pan Lu, Liang Qiu, Kai-Wei Chang, Ying Nian Wu, Song-Chun Zhu, Tanmay Rajpurohit, Peter Clark, and Ashwin Kalyan. Dynamic prompt learning via policy gradient for semi-structured mathematical reasoning. In *ICLR*, 2023.
- Shen-Yun Miao, Chao-Chun Liang, and Keh-Yih Su. A diverse corpus for evaluating and developing english math word problem solvers. In *Proceedings of the 58th Annual Meeting of the Association for Computational Linguistics*, pp. 975–984, 2020.
- Arkil Patel, Satwik Bhattamishra, and Navin Goyal. Are nlp models really able to solve simple math word problems? In *Proceedings of the 2021 Conference of the North American Chapter of the Association for Computational Linguistics: Human Language Technologies*, pp. 2080–2094, 2021.
- Ziqing Qiao, Yongheng Deng, Jiali Zeng, Dong Wang, Lai Wei, Fandong Meng, Jie Zhou, Ju Ren, and Yaoxue Zhang. Concise: Confidence-guided compression in step-by-step efficient reasoning. *arXiv preprint arXiv:2505.04881*, 2025.
- Corrado Rainone, Tim Bakker, and Roland Memisevic. Replacing thinking with tool usage enables reasoning in small language models. *arXiv preprint arXiv:2507.05065*, 2025.
- Olivier Roy and Martin Vetterli. The effective rank: A measure of effective dimensionality. In *2007 15th European signal processing conference*, pp. 606–610. IEEE, 2007.
- John Schulman, Philipp Moritz, Sergey Levine, Michael Jordan, and Pieter Abbeel. High-dimensional continuous control using generalized advantage estimation. *arXiv preprint arXiv:1506.02438*, 2015.
- John Schulman, Filip Wolski, Prafulla Dhariwal, Alec Radford, and Oleg Klimov. Proximal policy optimization algorithms. *arXiv preprint arXiv:1707.06347*, 2017.
- Zhihong Shao, Peiyi Wang, Qihao Zhu, Runxin Xu, Junxiao Song, Mingchuan Zhang, Y.K. Li, Y. Wu, and Daya Guo. Deepseekmath: Pushing the limits of mathematical reasoning in open language models, 2024. URL <https://arxiv.org/abs/2402.03300>.

- Guangming Sheng, Chi Zhang, Zilingfeng Ye, Xibin Wu, Wang Zhang, Ru Zhang, Yanghua Peng, Haibin Lin, and Chuan Wu. Hybridflow: A flexible and efficient rlhf framework. In *Proceedings of the Twentieth European Conference on Computer Systems*, pp. 1279–1297, 2025.
- Oscar Skean, Md Rifat Arefin, Dan Zhao, Niket Patel, Jalal Naghiyev, Yann LeCun, and Ravid Shwartz-Ziv. Layer by layer: Uncovering hidden representations in language models. *arXiv preprint arXiv:2502.02013*, 2025.
- Shenzhi Wang, Le Yu, Chang Gao, Chujie Zheng, Shixuan Liu, Rui Lu, Kai Dang, Xionghui Chen, Jianxin Yang, Zhenru Zhang, et al. Beyond the 80/20 rule: High-entropy minority tokens drive effective reinforcement learning for llm reasoning. *arXiv preprint arXiv:2506.01939*, 2025.
- Tianwen Wei, Jian Luan, Wei Liu, Shuang Dong, and Bin Wang. Cmath: Can your language model pass chinese elementary school math test? *CoRR*, 2023.
- Thomas Wolf, Lysandre Debut, Victor Sanh, Julien Chaumond, Clement Delangue, Anthony Moi, Pierric Cistac, Tim Rault, Rémi Louf, Morgan Funtowicz, et al. Huggingface’s transformers: State-of-the-art natural language processing. *arXiv preprint arXiv:1910.03771*, 2019.
- Hang Yan, Fangzhi Xu, Rongman Xu, Yifei Li, Jian Zhang, Haoran Luo, Xiaobao Wu, Luu Anh Tuan, Haiteng Zhao, Qika Lin, et al. Mur: Momentum uncertainty guided reasoning for large language models. *arXiv preprint arXiv:2507.14958*, 2025.
- An Yang, Baosong Yang, Binyuan Hui, Bo Zheng, Bowen Yu, Chang Zhou, Chengpeng Li, Chengyuan Li, Dayiheng Liu, Fei Huang, et al. Qwen2 technical report. *arXiv preprint arXiv:2407.10671*, 2024.
- Qiyang Yu, Zheng Zhang, Ruofei Zhu, Yufeng Yuan, Xiaochen Zuo, Yu Yue, Tiantian Fan, Gaohong Liu, Lingjun Liu, Xin Liu, et al. Dapo: An open-source llm reinforcement learning system at scale. *CoRR*, 2025.
- Yang Yue, Zhiqi Chen, Rui Lu, Andrew Zhao, Zhaokai Wang, Shiji Song, and Gao Huang. Does reinforcement learning really incentivize reasoning capacity in llms beyond the base model? *arXiv preprint arXiv:2504.13837*, 2025.
- Weihao Zeng, Yuzhen Huang, Qian Liu, Wei Liu, Keqing He, Zejun Ma, and Junxian He. Simplerl-zoo: Investigating and taming zero reinforcement learning for open base models in the wild, 2025. URL <https://arxiv.org/abs/2503.18892>.
- Beichen Zhang, Kun Zhou, Xilin Wei, Xin Zhao, Jing Sha, Shijin Wang, and Ji-Rong Wen. Evaluating and improving tool-augmented computation-intensive math reasoning. *Advances in Neural Information Processing Systems*, 36:23570–23589, 2023.
- Yuxin Zuo, Kaiyan Zhang, Li Sheng, Shang Qu, Ganqu Cui, Xuekai Zhu, Haozhan Li, Yuchen Zhang, Xinwei Long, Ermo Hua, et al. Ttrl: Test-time reinforcement learning. *arXiv preprint arXiv:2504.16084*, 2025.

CONTENTS OF APPENDIX

A	Notations	16
B	Algorithm	17
C	Details of Theorems	17
C.1	Proof of Theorem 3.1	17
C.2	Proof of Proposition 3.5	18
D	Implementation Details	20
D.1	Training and Evaluation Details	20
D.2	Efficient Incremental Computation of Higher-Order Metrics	20
D.3	Time Overhead of VERL Training	21
E	More Experiments	22
E.1	Analysis of Response-Level Hidden States	22
E.2	Analysis of Dataset-Level Hidden States	23
E.3	Detailed Analysis of Pass@1 Performance	26
E.4	Detailed Analysis of Pass@ k Performance	27
F	Case Study	28
F.1	Case Study For Pass@1 Setting	28
F.2	Case Study For Pass@16 Setting	29

A NOTATIONS

Symbol	Description
π	Large language model policy
$A_{i,t}$	Group-relative advantage for the t -th token in the i -th response in group
$A^{(0)}$	Original advantage estimation
\hat{A}	Reshaped advantage value
z_t	Hidden state corresponding to the t -th step of the output token
\bar{z}_i	Single vector representation for the i -th response by averaging its token hidden states
\mathbf{Z}_c	Mean-centered hidden state matrix
$\bar{\mathbf{Z}}_{1:n}$	Dataset-level hidden states matrix formed by the first n prompts
\mathbf{Z}	Response-level hidden states matrix
$\Delta_M^{(i)}$	The i -order temporal difference for metric M
\mathcal{M}	Set of metrics derived from the hidden states
M_i	T -order temporal difference of ER, exactly the different metrics
m_t	Value of metric M computed on the token sub-sequence from the start to position t
$\epsilon_{\text{high/low}}$	Hyperparameter for the upper/lower bound used for clipping
ϵ	Small constant for numerical stability
r_j	Reward of the j -th response
$\mathbf{w}_{\text{explore/exploit/dyn}}$	Exploration-focused profile/Exploitation-focused profile/Dynamic-weighted profile
$w_{\text{dyn},i}$	The i -th scalar of $\mathbf{w}_{\text{dynamic}}$
$\text{rank}(\cdot)/\text{erank}(\cdot)$	Conventional rank/Effective rank function
$\text{SVD}(\cdot)$	a function to calculate the singular values
$\delta_n^{(i)}$	Instantaneous i -Order Difference for step n
s	The stride for effective rank velocity calculation
y_t	The t -th step (token) of the model's response
$y_{i:j}$	Sequence of reasoning steps from i to j
$\bar{\mu}_k$	Exponential Moving Average for metric M_k
$\lambda_j(\cdot)$	The j -th eigenvalues of the given matrix
β	Interpolation coefficient for VERL training
G	Size of sampled group in GRPO
θ	Large language model policy's parameter
ϕ	The parameter corresponding to the optimal policy
Φ	Auxiliary advantage
t	Time step
T	Output length
L_{max}	The maximum length of model's output
x	Prompt
S	Sample times per prompt
\mathcal{P}_x	Distribution of prompts
ρ_t	Probability ratio between the current and old policies for t -step of the output
p_j	The j -th normalized singular values
$\mathcal{L}_{\text{PPO}}(\cdot)$	The optimization objective for PPO applied to policy
D	Feature dimension of hidden states
N	The size of the dataset
σ_j	The j -th singular value of matrix
\mathbf{P}	Singular value distribution
\mathcal{T}	Set of time steps
d_k	Deviation for metric M_k
κ	Advantage clipping factor
Δ	Performance difference between the baseline RL method and its VERL variant
$H(\cdot)$	Shannon entropy function
\mathbf{q}_i	The i -th row of the dataset matrix
$\bar{\mathbf{K}}$	Gram matrix of dataset matrix
U_t	Uncentered Gram matrix

B ALGORITHM

Algorithm 1 VRL: Training

- 1: **Input:** $\mathcal{D} = \{x^i\}_{i=1}^N$, prompt x^i , policy model π_θ , hidden-state dimension D , sample times per prompt S .
- 2: **Parameters:** EMA factor γ , relative deviation stabilizing factor $\epsilon \ll 1$, RL fine-tuning stabilizing factor κ .
- 3: **Initialize:** Randomly initialize policy parameters π_θ , historical averages of metrics $\bar{\mu}_{\text{ER}} = \bar{\mu}_{\text{ERV}} = \bar{\mu}_{\text{ERA}} = 0$, exploration capacity profile $\mathbf{w}_{\text{explore}} = [1, 0]$, exploitation capacity profile $\mathbf{w}_{\text{exploit}} = [0, 1]$.
- 4: **Output:** A well-trained policy model π_θ .
- 5: **repeat**
- 6: **for** $x^i \in \mathcal{D}$ **do:** // Pick a sample from dataset
- 7: **for** 1 **to** S **do:** // Rolling S times for one sample
- 8: $y_0^i \leftarrow x^i, \mathbf{Z}_0^i \leftarrow \emptyset, t \leftarrow 1$
- 9: **repeat** // Generation process
- 10: $y_t^i, \mathbf{z}_t^i \sim \pi_\theta(\cdot | y_{t-1}^i)$
- 11: $y_t^i \leftarrow [y_{t-1}^i; y_t^i]$ // Concatenate token sequence
- 12: $\mathbf{Z}_t^i \leftarrow [\mathbf{Z}_{t-1}^i; \mathbf{z}_t^i] \in \mathbb{R}^{t \times D}$
- 13: $\boldsymbol{\sigma}_t^i \leftarrow \text{SVD}(\mathbf{Z}_t^i)$
- 14: $j \leftarrow |\boldsymbol{\sigma}_t^i|$
- 15: $p_{j,t}^i \leftarrow \sigma_{j,t}^i / \sum_j \sigma_{j,t}^i$
- 16: $\text{erank}_t^i \leftarrow \exp\left(-\sum_j p_{j,t}^i \log p_{j,t}^i\right)$
- 17: **If** $t > 1$ **then:** $\delta_{\text{ERV},t} \leftarrow \text{erank}_t^i - \frac{1}{t-1} \sum_{k=1}^{t-1} \text{erank}_k^i$
- 18: **If** $t > 2$ **then:** $\delta_{\text{ERA},t} \leftarrow \delta_{\text{ERV},t} - \delta_{\text{ERV},t-1}$
- 19: $t \leftarrow t + 1$
- 20: **until** rolling done the sentence; // $t - 1$ is the final timestep while rolling done
- 21: $A_{\text{origin}}^i \leftarrow$ base RL evaluating on y_{t-1}^i
- 22: $m_{\text{ER}}^i \leftarrow \text{erank}_{t-1}^i$ // Calculating ER metric
- 23: $m_{\text{ERV}}^i \leftarrow \frac{1}{t-2} \sum_{t=2}^{t-1} \delta_{\text{ERV}}^t$ // Calculating ERV metric
- 24: $m_{\text{ERA}}^i \leftarrow \frac{1}{t-3} \sum_{t=3}^{t-1} \delta_{\text{ERA}}^t$ // Calculating ERA metric
- 25: $\bar{\mu}_k \leftarrow \gamma \bar{\mu}_k + (1 - \gamma) m_k^i, k \in \{\text{ER}, \text{ERV}, \text{ERA}\}$
- 26: $d_k^i \leftarrow \frac{m_k^i - \bar{\mu}_k}{|\bar{\mu}_k| + \epsilon}, k \in \{\text{ER}, \text{ERV}, \text{ERA}\}$
- 27: $\beta^i \leftarrow \text{sigmoid}(d_{\text{ERA}}^i)$
- 28: $\mathbf{w}_{\text{dyn}}^i \leftarrow \beta^i \mathbf{w}_{\text{explore}} + (1 - \beta^i) \mathbf{w}_{\text{exploit}}$
- 29: $w_{\text{dyn,ER}}^i \leftarrow$ the first scalar value of $\mathbf{w}_{\text{dyn}}^i$
- 30: $w_{\text{dyn,ERV}}^i \leftarrow$ the second scalar value of $\mathbf{w}_{\text{dyn}}^i$
- 31: $\Phi^i \leftarrow w_{\text{dyn,ER}}^i \tanh(d_{\text{ER}}^i) + w_{\text{dyn,ERV}}^i \tanh(d_{\text{ERV}}^i)$
- 32: $\hat{A}^i \leftarrow A_{\text{origin}}^i + \min\left(\max(0, \Phi^i), \frac{|A_{\text{origin}}^i|}{\kappa}\right)$
- 33: **end for**
- 34: **end for**
- 35: Update θ via base RL objective with \hat{A}^i
- 36: **until** θ converges;

C DETAILS OF THEOREMS

C.1 PROOF OF THEOREM 3.1

Suppose we have a matrix of embeddings $\mathbf{Z} \in \mathbb{R}^{T \times D}$. Then the effective rank of \mathbf{Z} is a lower bound of $\text{rank}(\mathbf{Z})$:

$$1 \leq \text{erank}(\mathbf{Z}) \leq \text{rank}(\mathbf{Z}) \leq \min\{T, D\} \quad (12)$$

Proof. Let the singular value distribution of the matrix \mathbf{Z} be $\mathbf{p} = (p_1, p_2, \dots, p_{\min\{T, D\}})$. The Shannon entropy of this distribution $H(\mathbf{p})$ is bounded. Its minimum is 0, which occurs when only one element of \mathbf{p} is 1 and all others are 0. Its maximum is $\log k$, where k is the number of non-zero singular values, and this occurs when the distribution is uniform ($p_j = 1/k$ for all non-zero values). The lower bound is established from the minimum entropy value:

$$\text{erank}(\mathbf{Z}) = \exp(H(\mathbf{p})) \geq \exp(0) = 1 \quad (13)$$

Equality holds if and only if the singular value distribution is $(1, 0, \dots, 0)$, meaning \mathbf{Z} has only one non-zero singular value. For the upper bound, let $k = \text{rank}(\mathbf{Z})$ be the number of non-zero singular values of \mathbf{Z} . The entropy of the distribution p is calculated only over these k values and is maximized when they are uniform. Therefore

$$H(\mathbf{p}) \leq \log k \quad (14)$$

Applying the exponential function to this inequality gives:

$$\text{erank}(\mathbf{Z}) = \exp(H(\mathbf{p})) \leq \exp(\log k) = k = \text{rank}(\mathbf{Z}) \quad (15)$$

This establishes that the effective rank is upper-bounded by the conventional rank. The final inequality, $\text{rank}(\mathbf{Z}) \leq \min\{T, D\}$, is a standard property of matrix rank. Equality for $\text{erank}(\mathbf{Z}) = \text{rank}(\mathbf{Z})$ holds if and only if the non-zero singular values are all equal, corresponding to a uniform singular value distribution over its support.

C.2 PROOF OF PROPOSITION 3.5

The zero-order metric and first-order difference of the effective rank scales linearly with the number of responses, $\Delta_M^{(0)} = \mathcal{O}(N)$, $\Delta_M^{(1)} = \mathcal{O}(N)$. The second-order difference of the effective rank is constant and does not depend on N , yielding a scaling order of $\Delta_M^{(2)} = \mathcal{O}(1)$.

Proof. Without loss of generality, we take the effective rank for example. We adopt the provided definition of effective rank for a representation matrix \mathbf{Z} with singular values $\{\sigma_i\}$:

$$\text{erank}(\mathbf{Z}) = \exp\left(-\sum_j p_j \log(p_j)\right), \quad \text{where } p_j = \frac{\sigma_j}{\sum_k \sigma_k} \quad (16)$$

Our analysis focuses on the dataset matrix $\bar{\mathbf{Z}} \in \mathbb{R}^{N \times D}$, whose rows $\{\mathbf{q}_i\}_{i=1}^N$ are the mean token embeddings of N responses. The singular values $\sigma_j(\bar{\mathbf{Z}})$ of $\bar{\mathbf{Z}}$ are the square roots of the eigenvalues of the Gram matrix $\bar{\mathbf{K}} = \bar{\mathbf{Z}}\bar{\mathbf{Z}}^\top$; i.e., $\sigma_j(\bar{\mathbf{Z}}) = \sqrt{\lambda_j(\bar{\mathbf{K}})}$. Given that the rows of $\bar{\mathbf{Z}}$ are nearly orthogonal, the Gram matrix $\bar{\mathbf{K}}$ is strongly diagonal-dominant. Its eigenvalues can be approximated by its diagonal entries:

$$\lambda_j(\bar{\mathbf{K}}) \approx \bar{\mathbf{K}}_{jj} = \|\mathbf{q}_j\|^2 = \frac{1}{T} \quad \text{for } j = 1, \dots, N \quad (17)$$

The matrix has N significant eigenvalues, each approximately equal to $1/T$. The singular values of $\bar{\mathbf{Z}}$ are the square roots of the eigenvalues of $\bar{\mathbf{K}}$:

$$\sigma_j(\bar{\mathbf{Z}}) = \sqrt{\lambda_j(\bar{\mathbf{K}})} \approx \sqrt{\frac{1}{T}} = \frac{1}{\sqrt{T}} \quad \text{for } j = 1, \dots, N \quad (18)$$

To calculate the effective rank, we first normalize these singular values to form a probability distribution $\{p_j\}$. The sum of singular values is:

$$\sum_{k=1}^N \sigma_k(\bar{\mathbf{Z}}) \approx \sum_{k=1}^N \frac{1}{\sqrt{T}} = \frac{N}{\sqrt{T}} \quad (19)$$

The individual probabilities are therefore:

$$p_j = \frac{\sigma_j}{\sum_k \sigma_k} \approx \frac{1/\sqrt{T}}{N/\sqrt{T}} = \frac{1}{N} \quad (20)$$

The distribution $\mathbf{p} = \{p_1, p_2, \dots, p_N\}$ is a uniform distribution over N states. The Shannon entropy of this distribution is maximal:

$$H(\mathbf{p}) = - \sum_{j=1}^N p_j \log(p_j) = - \sum_{j=1}^N \frac{1}{N} \log\left(\frac{1}{N}\right) = -N \left(\frac{-\log(N)}{N}\right) = \log(N) \quad (21)$$

The effective rank is the exponential of this entropy: $\text{erank}(\bar{\mathbf{Z}}) = \exp(H(\mathbf{p})) = \exp(\log(N)) = N$. In the maximal prompt entropy regime, the effective rank of the dataset matrix scales as $\mathcal{O}(N)$.

We adapt them to our context by defining the metric's value at "time" n as the Effective Rank computed on the dataset matrix formed by the first n prompts, denoted $\bar{\mathbf{Z}}_{1:n}$. Let $m_n = \text{erank}(\bar{\mathbf{Z}}_{1:n})$. From our previous analysis, we established a crucial result that forms the basis of this derivation: for maximal cases, the effective rank of a dataset with n prompts scales linearly with n .

$$m_n = \text{erank}(\bar{\mathbf{Z}}_{1:n}) \approx n \quad (22)$$

We will use this linear approximation to derive the scaling orders of the difference metrics, assuming a stride of $s = 1$ for simplicity. The first-order difference quantifies the average "velocity" of change in the metric relative to its historical mean. Instantaneous First-Order Difference ($\delta_n^{(1)}$) is the value at step n minus the average of all preceding values.

$$\delta_n^{(1)} = m_n - \left(\frac{1}{n-1} \sum_{k=1}^{n-1} m_k \right) \quad (23)$$

Substituting our approximation $m_k \approx k$:

$$\delta_n^{(1)} \approx n - \left(\frac{1}{n-1} \sum_{k=1}^{n-1} k \right) \quad (24)$$

$$\delta_n^{(1)} \approx n - \left(\frac{1}{n-1} \cdot \frac{(n-1)n}{2} \right) = n - \frac{n}{2} = \frac{n}{2} \quad (25)$$

The instantaneous difference grows linearly with n . Overall First-Order Difference $\Delta_{\text{erank}}^{(1)}$: This is the average of the instantaneous differences over the entire dataset of size N .

$$\Delta_{\text{erank}}^{(1)} = \frac{1}{N-1} \sum_{n=2}^N \delta_n^{(1)} \approx \frac{1}{N-1} \sum_{n=2}^N \frac{n}{2} \quad (26)$$

$$\Delta_{\text{erank}}^{(1)} \approx \frac{1}{2(N-1)} \left(\left(\sum_{n=1}^N n \right) - 1 \right) = \frac{1}{2(N-1)} \left(\frac{N(N+1)}{2} - 1 \right) \quad (27)$$

For large N , the expression is dominated by the highest power of N :

$$\Delta_{\text{erank}}^{(1)} \sim \frac{N^2/4}{N} = \frac{N}{4} \quad (28)$$

The first-order difference of the effective rank scales linearly with the number of prompts, $\Delta_{\text{erank}}^{(1)} = \mathcal{O}(N)$. As for second-order difference, we compute the change in Instantaneous Differences between consecutive values of $\delta_n^{(1)}$.

$$\delta_n^{(1)} - \delta_{n-1}^{(1)} \approx \frac{n}{2} - \frac{n-1}{2} = \frac{1}{2} \quad (29)$$

This change is a constant, indicating a linear increase in the first-order difference. Overall Second-Order Difference $\Delta_{\text{erank}}^{(2)}$:

$$\Delta_{\text{erank}}^{(2)} = \frac{1}{N-2} \sum_{n=3}^N (d_n^{(1)} - d_{n-1}^{(1)}) \approx \frac{1}{N-2} \sum_{n=3}^N \frac{1}{2} \quad (30)$$

$$\Delta_{\text{erank}}^{(2)} \approx \frac{1}{N-2} \cdot (N-2) \cdot \frac{1}{2} = \frac{1}{2} \quad (31)$$

The second-order difference of the effective rank is constant and does not depend on N , yielding a scaling order of $\Delta_{\text{erank}}^{(2)} = \mathcal{O}(1)$.

D IMPLEMENTATION DETAILS

D.1 TRAINING AND EVALUATION DETAILS

We typically use the same set of hyperparameters to train and evaluate all models in the SimpleRL-Zoo series (Zeng et al., 2025) in the default main experiment setting.

Training. We conduct all experiments with 4 A800-PCIE-80GB GPUs. For GRPO and PPO, we use a prompt batch size of 48 with a maximum rollout length of 1536 tokens. Training is performed using a mini-batch size of 24. For GRPO, we generate 4 rollouts per prompt. For PPO, we use DeepSeek-R1-Distill-Qwen-1.5B (Guo et al., 2025) as the value model and generate 1 rollout per prompt. The default sampling temperature is set to 1.0, and the clip ratio is 0.2. For all actor models ranging from 3B to 8B parameters, we use a learning rate of 1e-6 and a KL loss coefficient of 1e-4. For critic models in PPO, we use a learning rate of 1e-5. For our training datasets, we follow the same setup as in Zeng et al. (2025), where the data is filtered from GSM8K (Cobbe et al., 2021) and MATH (Hendrycks et al., 2021) configured with different difficulty levels for models of varying capabilities. We tested using the checkpoint model trained up to 120 steps.

Evaluation. We build our evaluation script based on that of Zeng et al. (2025), using a temperature of 0.6 and a maximum generation length of 2048 tokens. To ensure consistency, we adopt the same prompt template used during training. For most benchmarks, we report Pass@1 results. However, for benchmarks like AIME 2024, which contains fewer problems, we report both Pass@1 and average accuracy (Pass@256), computed over 256 generated samples per problem.

Base Models. To demonstrate the universality of our insights and methods, we conduct zero RL training experiments on Llama-3.2 (3B), Llama-3.1 (8B) (Dubey et al., 2024), Mistral-v0.3-7B (Jiang et al., 2024), and Qwen-2.5 (1.5B, 3B, 7B) (Hui et al., 2024). For value model in PPO, we use DeepSeek-R1-Distill-Qwen-1.5B (Guo et al., 2025) for all experiments. These models were loaded and handled using the Hugging Face transformers library (Wolf et al., 2019), which provided a robust framework for our training and inference pipeline.

Benchmark. We evaluate on a diverse suite of mathematical reasoning benchmarks. These include standard benchmarks such as GSM8K (Cobbe et al., 2021), MATH (Hendrycks et al., 2021), AS-Div (Miao et al., 2020), Carp (English Version) (Zhang et al., 2023), MAWPS (Koncel-Kedziorski et al., 2016), SVAMP (Patel et al., 2021), TabMWP (Lu et al., 2023), and OlympiadBench (He et al., 2024); Chinese mathematics collections like CMATH (Wei et al., 2023) and Gaokao 2024; and benchmarks from mathematics competitions, including the 2024/2025 AIME and the 2023/2024 AMC.

D.2 EFFICIENT INCREMENTAL COMPUTATION OF HIGHER-ORDER METRICS

A naive computation of the temporal difference metrics would be computationally prohibitive. Our method’s feasibility hinges on an efficient, incremental algorithm that computes the required metrics without redundant operations on the growing hidden state matrix $\mathbf{Z} \in \mathbb{R}^{T \times D}$.

The effective rank is derived from the singular values of the mean-centered hidden state matrix \mathbf{Z}_c . These are equivalent to the square roots of the eigenvalues of the centered Gram matrix $G = \mathbf{Z}_c \mathbf{Z}_c^\top$. Instead of recomputing G_t from scratch at each time step t , our algorithm incrementally updates two sufficient statistics: the uncentered Gram matrix $U_t = \mathbf{Z}_{1:t} \mathbf{Z}_{1:t}^\top$ and the sum of hidden state vectors $s_t = \sum_{i=1}^t z_i$. When extending the analysis window, the new uncentered Gram matrix U_t is

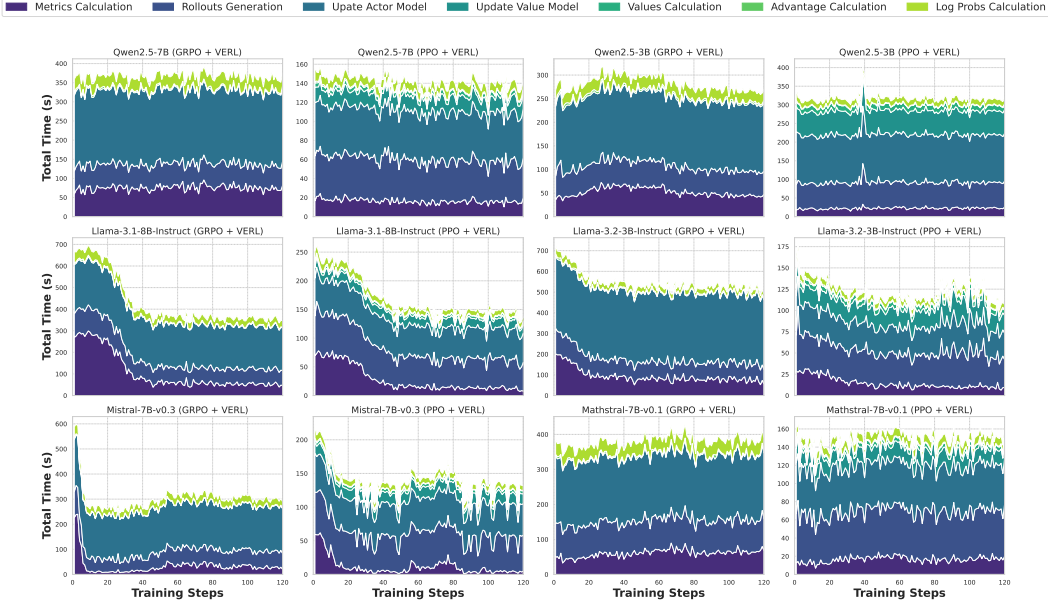


Figure 7: Time overhead of the main computation of RL Training.

constructed from the prior matrix U_{t-s} and the new chunk of hidden states $\Delta Z_t = Z_{t-s+1:t}$. This update follows a recursive block matrix structure:

$$U_t = \begin{pmatrix} U_{t-s} & Z_{1:t-s}(\Delta Z_t)^\top \\ (\Delta Z_t)Z_{1:t-s}^\top & (\Delta Z_t)(\Delta Z_t)^\top \end{pmatrix} \quad (32)$$

From the efficiently updated U_t and s_t , we can directly construct the centered Gram matrix G_t . Letting $\boldsymbol{\mu}_t = s_t/t$ be the mean vector and $\mathbf{1}_t$ be a column vector of ones, G_t can be expressed as:

$$G_t = U_t - (Z_{1:t}\boldsymbol{\mu}_t)\mathbf{1}_t^\top - \mathbf{1}_t(Z_{1:t}\boldsymbol{\mu}_t)^\top + (\boldsymbol{\mu}_t^\top \boldsymbol{\mu}_t) \cdot (\mathbf{1}_t\mathbf{1}_t^\top) \quad (33)$$

This allows for the calculation of G_t without re-accessing the full history of hidden states. The eigenvalues $\{\lambda_j\}$ of G_t are then used to derive the effective rank. First, the singular values of the centered matrix are obtained, $\sigma_j = \sqrt{\lambda_j}$. These are normalized to form a probability distribution, $p_j = \sigma_j / \sum_k \sigma_k$. The effective rank is then the exponential of the Shannon entropy of this distribution: $\text{erank}(Z_{c,t}) = \exp\left(-\sum_j p_j \log p_j\right)$. This pipeline efficiently yields a sequence of effective rank values, $m_{j,s} = \text{erank}(Z_{c,j,s})$, at each stride s . From this sequence, we compute the instantaneous first-order difference, δ , which compares the current value to the running average of all preceding values. This is defined recursively as: $\delta_{j,s} = m_{j,s} - \frac{1}{j-1} \sum_{k=1}^{j-1} m_{k,s}$.

The computational advantage of this incremental approach is substantial. While the total cost for the series of eigenvalue decompositions $O(T^4/s)$, is common to both methods, the cost of matrix construction differs significantly. The naive method’s recalculation totals $O(DT^3/s)$, whereas our incremental update method reduces this to $O(DT^2)$. This reduction of the polynomial dependency on sequence length T from cubic to quadratic is critical, as this term is multiplied by the large hidden dimension D , making it the dominant factor in practical performance and rendering the dense calculation of temporal dynamics feasible.

D.3 TIME OVERHEAD OF VERL TRAINING

We conducted post-training with Zero RL on several base models. The Fig. 7 illustrates the time associated with each computational stage. The ‘metrics calculation’ component, which represents the cost of computing metrics for hidden states, accounts for an insignificant portion of the total processing time. This demonstrates that our method does not introduce substantial time overhead.

E MORE EXPERIMENTS

E.1 ANALYSIS OF RESPONSE-LEVEL HIDDEN STATES

As shown in Figs. 8 and 9, our analysis of response-level hidden states across additional LLMs confirms that the insights presented in Sec. 4.1 hold true for various base models and RL paradigms.

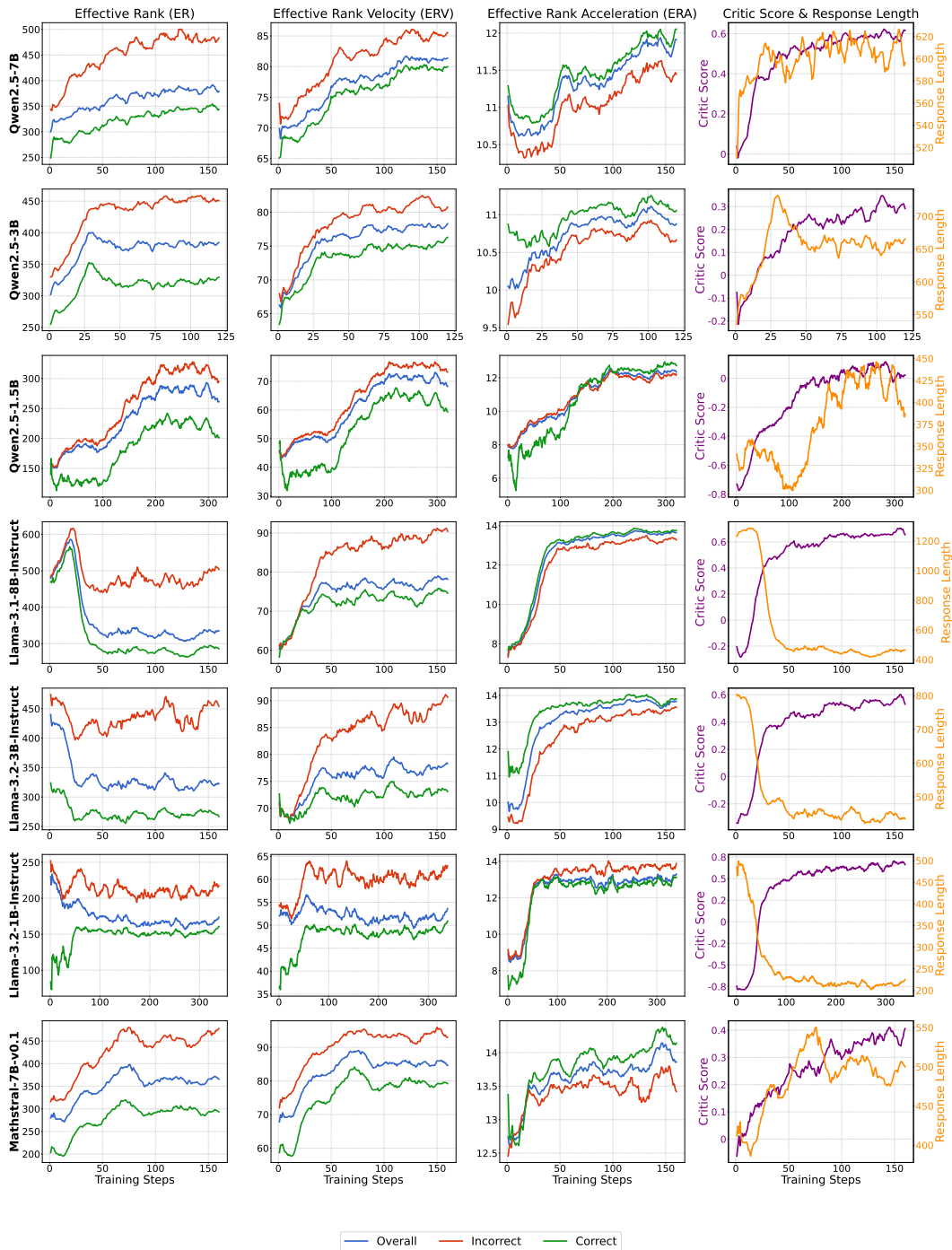


Figure 8: Visualization of response-level metrics for GRPO post-training. 'Overall' (blue) represents the metric across the entire data batch, while 'Correct' (green) and 'Incorrect' (red) show the metrics specifically for correctly and incorrectly classified samples, respectively. Data is smoothed using a rolling window of 10 steps to highlight underlying trends.

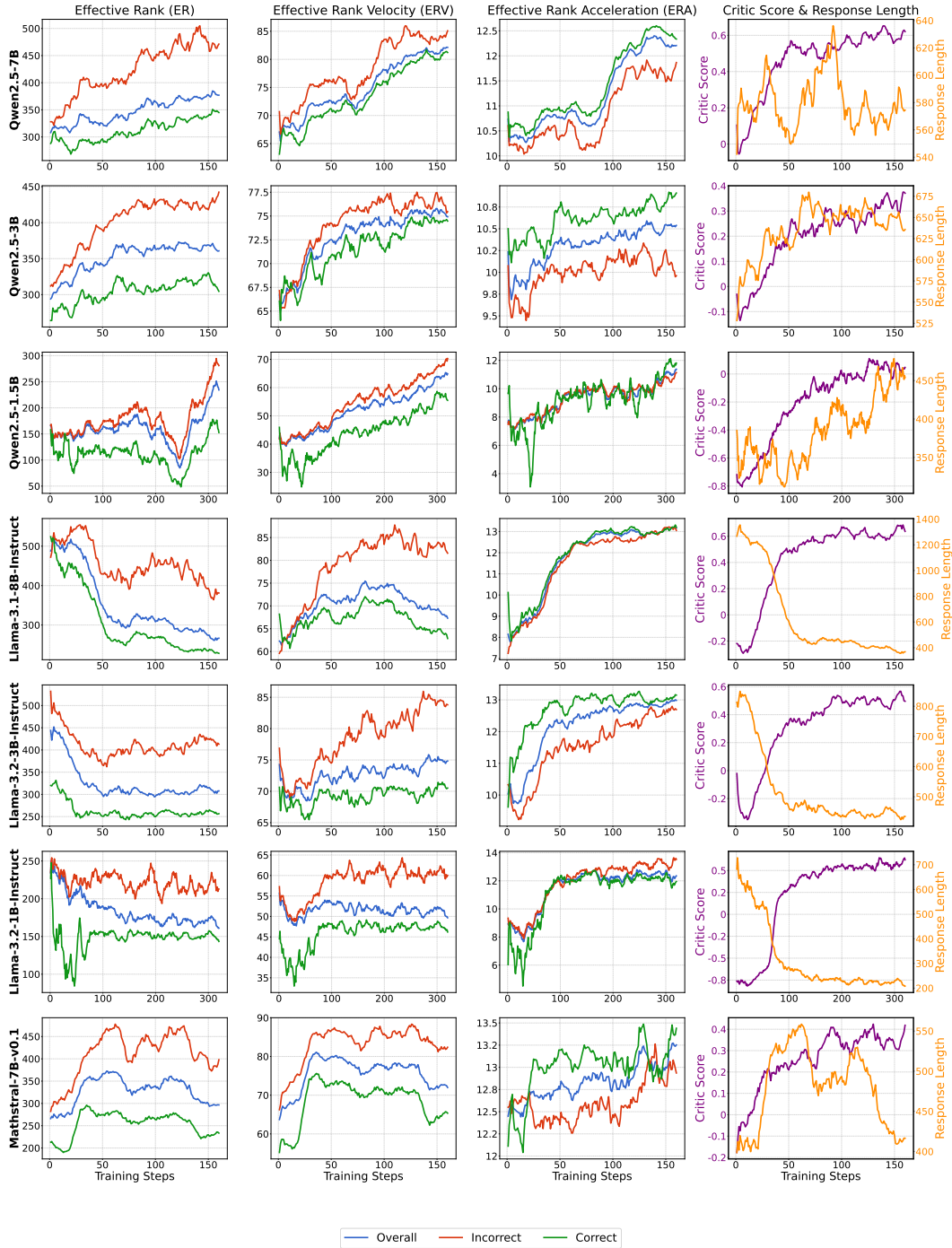


Figure 9: Visualization of response-level metrics for PPO post-training. 'Overall' (blue) represents the metric across the entire data batch, while 'Correct' (green) and 'Incorrect' (red) show the metrics specifically for correctly and incorrectly classified samples, respectively. Data is smoothed using a rolling window of 10 steps to highlight underlying trends.

E.2 ANALYSIS OF DATASET-LEVEL HIDDEN STATES

As shown in Figs. 10 and 11, our analysis of dataset-level hidden states across additional LLMs confirms that the insights presented in Sec. 4.2 hold for various base models and RL paradigms.

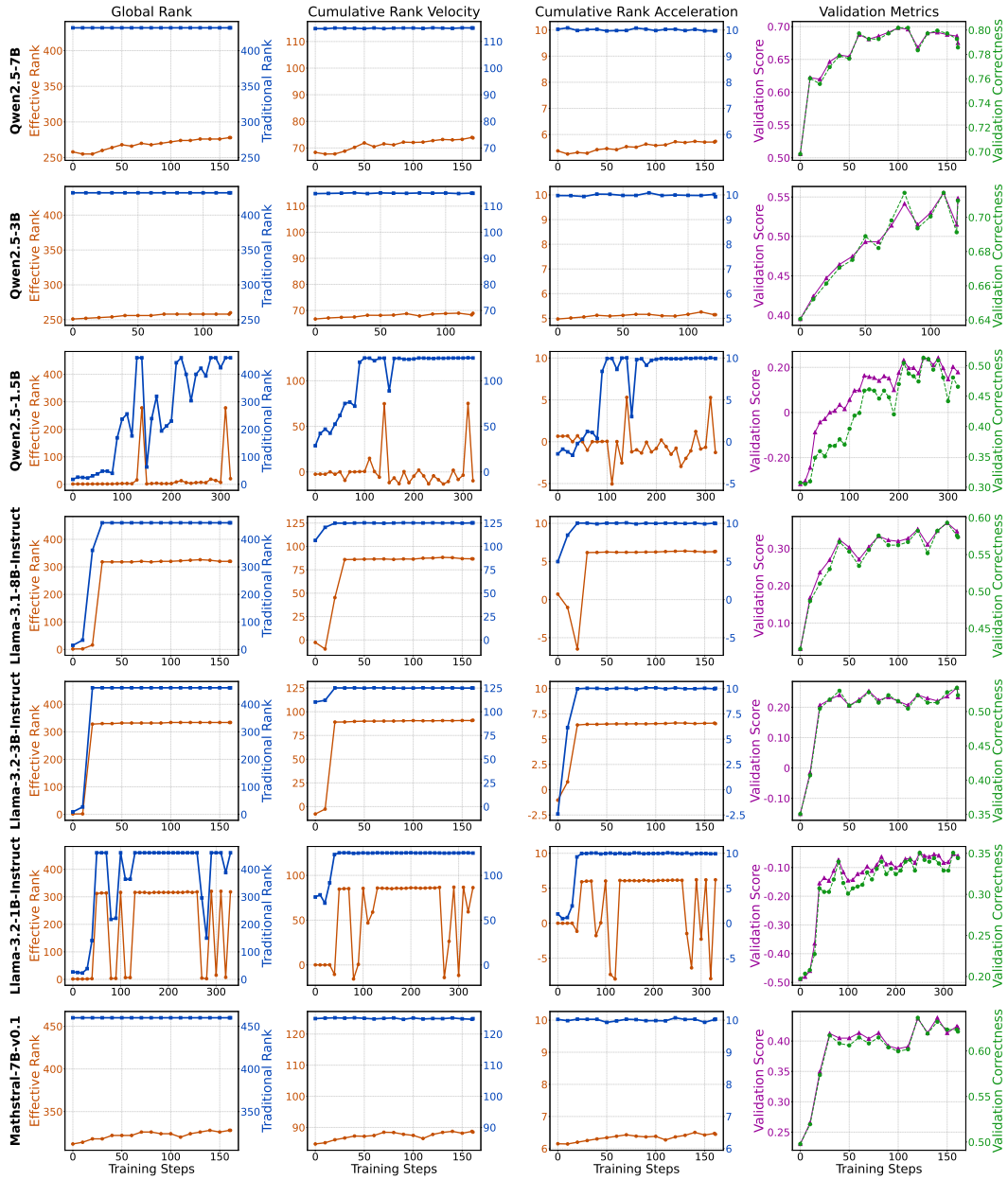


Figure 10: Visualization of dataset-level metrics for GRPO post-training

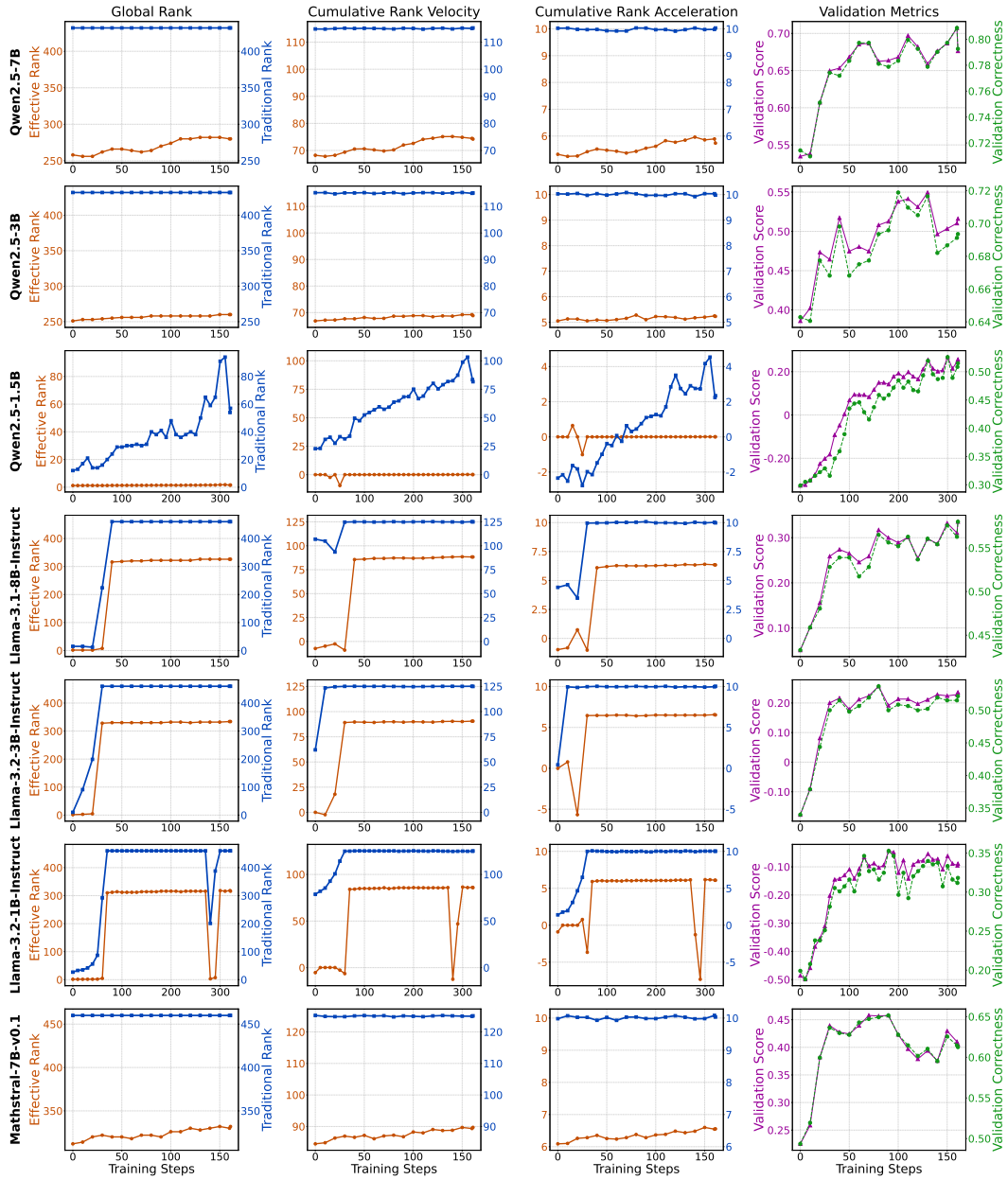


Figure 11: Visualization of dataset-level metrics for PPO post-training

E.3 DETAILED ANALYSIS OF PASS@1 PERFORMANCE

As shown in Tab. 4, Pass@1 measures the model’s ability to generate a correct answer in a single attempt, which directly reflects its exploitation ability. We fine-tune the base model by integrating our VERL-based Advantage method into two reinforcement learning paradigms, GRPO and PPO.

Table 4: Performance comparison of instruction-tuned models on mathematical reasoning benchmarks (Pass@1). “+ GRPO” and “+ PPO” denote reinforcement learning fine-tuning from the base model using GRPO and PPO, respectively. “w/ VERL.” indicates the application of our VERL-based advantage to the corresponding RL algorithm. Δ represents the performance difference between the baseline RL method and its VERL-advanced variant. All results are reported in percentage (%).

Model	AIME24	AIME25	AMC23	AMC24	ASDiv	Carp.En	CMATH	Gaokao 2024.I	Gaokao 2024.Mix	Gaokao MathCloze	GSM8K	MAWPS	Olympiad Bench	SVAMP	TabMWP	Avg.
Llama-3.2-3B-Instruct	0.0	0.0	25.0	11.1	74.6	26.5	10.2	14.3	14.3	6.8	66.6	86.9	12.7	74.1	41.4	31.0
+ GRPO	3.3	0.0	27.5	8.9	88.8	45.0	28.3	21.4	20.9	23.7	80.0	96.0	16.7	87.7	71.7	41.4
+ GRPO w/ VERL.	13.3	6.7	25.0	11.1	89.3	45.4	46.2	14.3	22.0	22.9	81.7	96.0	17.6	87.8	72.3	43.4
Δ_{GRPO}	+10.0	+6.7	-2.5	+2.2	+0.5	+0.4	+17.9	-7.1	+1.1	-0.8	+1.0	+0.0	+0.9	+0.1	+0.6	+2.0
+ PPO	10.0	3.3	22.5	13.3	87.9	46.4	21.2	7.1	16.5	20.3	81.4	95.5	17.8	86.8	71.0	40.1
+ PPO w/ VERL.	10.0	3.3	25.0	11.1	88.7	46.0	30.7	14.3	19.8	27.1	82.9	95.7	17.3	85.8	71.3	41.9
Δ_{PPO}	+0.0	+0.0	+2.5	-2.2	+0.8	-0.4	+9.5	+7.2	+3.3	+6.8	+1.5	+0.2	-0.5	-1.0	+0.3	+1.9
Llama-3.1-8B-Instruct	0.0	3.3	17.5	8.9	48.0	34.1	18.5	0.0	15.4	16.9	47.4	43.5	10.4	48.5	34.3	23.1
+ GRPO	6.7	0.0	22.5	15.6	90.3	42.4	60.7	7.1	14.3	32.2	88.4	96.4	19.7	88.5	82.7	44.5
+ GRPO w/ VERL.	10.0	3.3	32.5	15.6	90.7	45.0	72.7	14.3	14.3	30.5	88.6	96.9	21.3	88.4	83.1	47.2
Δ_{GRPO}	+3.3	+3.3	+10.0	+0.0	+0.4	+2.6	+12.0	+7.2	+0.0	-1.7	+0.2	+0.5	+1.6	-0.1	+0.4	+2.7
+ PPO	6.7	0.0	30.0	17.8	89.8	42.0	60.0	0.0	14.3	25.4	86.4	95.7	18.2	88.6	82.3	43.8
+ PPO w/ VERL.	10.0	0.0	35.0	13.3	90.7	42.6	62.0	14.3	22.0	28.8	87.3	96.6	19.1	88.1	83.0	46.2
Δ_{PPO}	+3.3	+0.0	+5.0	-4.5	+0.9	+0.6	+2.0	+14.3	+7.7	+3.4	+0.9	+0.9	+0.9	-0.5	+0.7	+2.4
Qwen2.5-3B	6.7	0.0	20.0	24.4	90.7	54.7	76.7	0.0	22.0	41.5	80.7	95.1	23.0	84.3	71.3	46.1
+ GRPO	3.3	0.0	40.0	22.2	92.6	56.0	82.7	7.1	27.5	42.4	82.8	96.6	23.6	89.0	81.4	49.8
+ GRPO w/ VERL.	6.7	0.0	30.0	17.8	92.6	56.9	84.8	21.4	33.0	49.2	82.2	96.4	24.4	88.5	81.0	51.0
Δ_{GRPO}	+0.0	-10.0	-4.4	+0.0	+0.9	+2.1	+14.3	+5.5	+6.8	-0.6	-0.2	+0.8	-0.5	-0.4	+1.2	
+ PPO	3.3	0.0	32.5	15.6	92.8	56.5	83.2	0.0	28.6	50.0	81.7	96.6	24.4	86.0	80.8	48.8
+ PPO w/ VERL.	6.7	0.0	32.5	17.8	92.6	57.0	84.3	21.4	29.7	47.5	81.8	96.5	24.6	88.3	81.4	50.8
Δ_{PPO}	+3.4	+0.0	+0.0	+2.2	-0.2	+0.5	+1.1	+21.4	+1.1	-2.5	+0.1	-0.1	+0.2	+2.3	+0.6	+2.0
Qwen2.5-7B	6.7	0.0	45.0	15.6	91.4	55.8	86.7	42.9	33.0	49.2	85.8	95.4	25.8	88.5	82.8	53.6
+ GRPO	10.0	6.7	55.0	26.7	94.8	60.2	91.7	14.3	34.1	64.4	90.2	97.6	36.1	92.8	91.3	57.7
+ GRPO w/ VERL.	13.3	10.0	50.0	28.9	95.0	60.8	90.7	35.7	35.2	69.5	89.2	97.7	35.4	92.9	91.9	59.8
Δ_{GRPO}	+3.3	+3.3	-5.0	+2.2	+0.2	+0.6	-1.0	+21.4	+1.1	+5.1	-1.0	+0.1	-0.7	+0.1	+0.6	+2.1
+ PPO	6.7	3.3	50.0	33.3	94.9	59.6	89.8	28.6	31.9	63.6	89.1	97.3	36.1	92.8	90.8	57.9
+ PPO w/ VERL.	10.0	6.7	52.5	33.3	94.8	60.0	90.3	28.6	34.1	66.9	90.2	97.8	36.1	92.5	90.6	59.0
Δ_{PPO}	+3.3	+3.3	+2.5	+0.0	-0.1	+0.4	+0.5	+0.0	+2.2	+3.3	+1.1	+0.5	+0.0	-0.3	-0.2	+1.1
Mathstral-7B-v0.1	0.0	0.0	12.5	8.9	87.1	51.1	74.2	28.6	33.0	31.4	81.6	93.8	17.9	87.7	54.7	44.2
+ GRPO	0.0	0.0	47.5	17.8	92.9	55.9	81.3	35.7	44.0	49.2	88.1	97.6	25.6	93.0	81.5	54.0
+ GRPO w/ VERL.	6.7	0.0	45.0	20.0	93.3	55.5	81.5	50.0	40.7	46.6	89.5	97.2	29.3	90.7	83.5	55.3
Δ_{GRPO}	+6.7	+0.0	-5.5	+2.2	+0.4	-0.4	+0.2	+14.3	-3.3	-2.6	+1.4	-0.4	+3.7	-2.3	+2.0	+1.3
+ PPO	6.7	3.3	32.5	20.0	90.9	51.8	78.3	42.9	37.4	49.2	87.0	96.0	28.4	89.9	70.7	52.3
+ PPO w/ VERL.	10.0	0.0	27.5	22.2	93.0	53.8	78.2	42.9	51.6	48.3	87.4	96.7	26.1	89.6	84.1	54.1
Δ_{PPO}	+3.3	-3.3	-5.0	+2.2	+2.1	+2.0	-0.1	+0.0	+14.2	-0.9	+0.4	+0.7	-2.3	-0.3	+13.4	+1.8
Mistral-7B-v0.3	0.0	0.0	10.0	0.0	40.5	12.4	21.8	14.3	13.2	3.4	24.0	50.8	1.6	39.1	30.6	17.4
+ GRPO	0.0	0.0	2.5	4.4	58.2	11.1	42.3	0.0	15.4	5.1	52.4	79.2	3.0	47.6	37.7	23.9
+ GRPO w/ VERL.	0.0	0.0	7.5	2.2	59.1	15.0	43.0	0.0	6.6	4.2	40.3	69.5	2.8	57.5	53.0	24.0
Δ_{GRPO}	+0.0	+0.0	+5.0	-2.2	+0.9	+3.9	+0.7	+0.0	-8.8	-0.9	-12.1	-9.7	-0.2	+9.9	+15.3	+0.1
+ PPO	0.0	0.0	0.0	0.0	8.9	6.6	7.7	7.1	11.0	2.5	3.3	8.6	2.1	6.9	12.0	5.1
+ PPO w/ VERL.	0.0	0.0	2.5	0.0	44.7	10.6	35.7	7.1	16.5	5.1	28.8	70.7	2.4	57.5	35.1	21.1
Δ_{PPO}	+0.0	+0.0	+2.5	+0.0	+35.8	+4.0	+28.0	+0.0	+5.5	+2.6	+25.5	+62.1	+0.3	+50.6	+23.1	+16.0

E.4 DETAILED ANALYSIS OF PASS@ k PERFORMANCE

As shown in Tab. 5, which provides a comprehensive analysis of the models’ performance on the Pass@ k metric, which is a direct measure of the model’s exploration ability. As a supplement to the main paper’s discussion, it presents the detailed performance of our VERL-based models across a variety of mathematical reasoning benchmarks. These results demonstrate that our method consistently leads to significant improvements, confirming its effectiveness in enhancing the models’ exploration capabilities.

Table 5: Performance comparison of instruction-tuned models under diverse decoding settings (Pass@ k). All results are reported in percentage (%).

Model	MATH500 (Pass@16)	AMC23 (Pass@128)	AMC24 (Pass@128)	AIME24 (Pass@256)	AIME25 (Pass@256)	Avg.
Llama-3.2-3B-Instruct	79.8	93.5	51.5	40.0	30.0	58.96
+ GRPO	80.2	95.4	60.6	40.0	30.0	61.24
+ GRPO w/ VERL.	80.6	95.7	59.0	50.0	36.7	64.40
Δ_{GRPO}	+0.4	+0.3	-1.6	+10.0	+6.7	+3.16
+ PPO	82.2	94.5	57.0	46.7	36.7	63.42
+ PPO w/ VERL.	82.4	94.7	57.8	46.7	40.0	64.32
Δ_{PPO}	+0.2	+0.2	+0.8	+0.0	+3.3	+0.90
Llama-3.1-8B-Instruct	79.8	94.6	57.4	46.7	36.7	63.04
+ GRPO	83.4	94.9	56.9	53.3	36.7	65.04
+ GRPO w/ VERL.	83.4	95.1	63.1	50.0	36.7	65.66
Δ_{GRPO}	+0.0	+0.2	+6.2	-3.3	+0.0	+0.62
+ PPO	79.2	92.4	59.0	46.7	36.7	62.80
+ PPO w/ VERL.	82.4	91.9	60.0	53.3	36.7	64.86
Δ_{PPO}	+3.2	-0.5	+1.0	+6.6	+0.0	+2.06
Qwen2.5-3B	86.0	96.7	69.0	56.7	40.0	69.68
+ GRPO	86.6	92.2	68.5	46.7	40.0	66.80
+ GRPO w/ VERL.	87.6	95.9	67.8	53.3	43.3	69.58
Δ_{GRPO}	+1.0	+3.7	-0.7	+6.6	+3.3	+2.78
+ PPO	87.8	96.5	67.9	43.3	43.3	67.76
+ PPO w/ VERL.	88.2	96.8	67.3	53.3	43.3	69.78
Δ_{PPO}	+0.4	+0.3	-0.6	+10.0	+0.0	+2.02
Qwen2.5-7B	90.6	98.4	73.7	60.0	60.0	76.54
+ GRPO	90.8	97.8	78.3	56.7	50.0	74.72
+ GRPO w/ VERL.	91.4	98.3	79.0	63.3	60.0	78.40
Δ_{GRPO}	+0.6	+0.5	+0.7	+6.6	+10.0	+3.68
+ PPO	91.2	98.6	74.3	53.3	56.7	74.82
+ PPO w/ VERL.	91.4	98.0	74.4	56.7	66.7	77.44
Δ_{PPO}	+0.2	-0.6	+0.1	+3.4	+10.0	+2.62
Mathstral-7B-v0.1	80.4	88.5	60.9	43.3	36.7	61.96
+ GRPO	84.8	87.3	69.2	36.7	40.0	63.60
+ GRPO w/ VERL.	87.0	97.0	76.9	50.0	50.0	72.18
Δ_{GRPO}	+2.2	+9.7	+7.7	+13.3	+10.0	+8.58
+ PPO	82.4	91.7	70.7	53.3	40.0	67.62
+ PPO w/ VERL.	84.8	93.8	69.9	53.3	46.7	69.70
Δ_{PPO}	+2.4	+2.1	-0.8	+0.0	+6.7	+2.08
Mistral-7B-v0.3	36.0	73.5	39.6	20.0	16.7	37.16
+ GRPO	33.0	63.2	36.0	10.0	10.0	30.44
+ GRPO w/ VERL.	34.4	64.5	38.0	16.7	13.3	33.38
Δ_{GRPO}	+1.4	+1.3	+2.0	+6.7	+3.3	+2.94
+ PPO	21.8	46.4	25.1	6.7	6.7	21.34
+ PPO w/ VERL.	19.2	46.5	30.1	3.3	13.3	22.48
Δ_{PPO}	-2.6	+0.1	+5.0	-3.4	+6.6	+1.14

F CASE STUDY

For all case studies presented in this section, we employ Qwen2.5-7B as the base model. The answers shown in the gray boxes are generated by Qwen2.5-7B trained with vanilla GRPO for 120 steps, while those in the purple boxes are produced by Qwen2.5-7B trained with GRPO augmented with the auxiliary shaping term—our proposed method VERL—for 120 steps.

F.1 CASE STUDY FOR PASS@1 SETTING

Case Study I. For the case shown in Fig. 12, the model trained with vanilla GRPO incorrectly judges $-1 < -13$, whereas the model trained with GRPO augmented with the auxiliary shaping term gives the correct answer. This example highlights the limitation of vanilla GRPO in exploitation: it fails to consistently apply basic numerical commonsense—namely, that larger absolute values correspond to smaller magnitudes for negative numbers. By contrast, introducing the Auxiliary Shaping Term strengthens exploitation capacity, enabling the model to make such comparisons more reliably.

Question

What is the smallest possible integer value of x if $12 \div (x + 1)$ is an integer?

Ground Truth

-13

Vanilla GRPO

To find the smallest possible integer value of x such that $\frac{12}{x+1}$ is an integer, we need to consider the factors of 12. The expression $\frac{12}{x+1}$ will be an integer if $x + 1$ is a divisor of 12. Let's list the divisors of 12:

- The divisors of 12 are: $\pm 1, \pm 2, \pm 3, \pm 4, \pm 6, \pm 12$.
- We need to find the smallest x , so we start with the smallest positive divisor, which is 1:

$$x + 1 = 1 \implies x = 1 - 1 \implies x = 0$$

- To confirm, we substitute $x = 0$ back into the original expression:

$$\frac{12}{0 + 1} = \frac{12}{1} = 12$$

Since 12 is an integer, $x = 0$ is indeed a valid solution.

- We should also consider the negative divisors to ensure we have the smallest possible integer value. The next smallest divisor is -1:

$$x + 1 = -1 \implies x = -1 - 1 \implies x = -2$$

- Substituting $x = -2$ back into the original expression:

$$\frac{12}{-2 + 1} = \frac{12}{-1} = -12$$

Since -12 is an integer, $x = -2$ is also a valid solution, but it is not smaller than $x = 0$.

Therefore, the smallest possible integer value of x is

0

GRPO with Auxiliary Shaping Term

To find the smallest possible integer value of x such that $\frac{12}{x+1}$ is an integer, we need to determine the divisors of 12. The divisors of 12 are $\pm 1, \pm 2, \pm 3, \pm 4, \pm 6, \pm 12$. For $\frac{12}{x+1}$ to be an integer, $x + 1$ must be one of these divisors. We want the smallest possible x , so we should consider the smallest positive divisor, which is 1.

If $x + 1 = 1$, then $x = 0$.

We should also consider the negative divisors to ensure we find the smallest possible integer value of x . The smallest negative divisor is -12. If $x + 1 = -12$, then $x = -13$.

Comparing $x = 0$ and $x = -13$, the smallest possible integer value of x is -13.

Therefore, the final answer is

-13

Figure 12: Case study: Vanilla GRPO fails to exploit numerical commonsense when comparing negative values (-1 vs. -13), while our method gives the correct answer.

Case Study II. For the case in Fig. 13, the crucial distinction lies in how the models interpret the condition “No house faces two different streets.” The vanilla GRPO-trained model incorrectly infers that each street contains only 10 houses, overlooking the structural implication of the condition. In contrast, the model trained with GRPO augmented by the auxiliary shaping term exploits this commonsense constraint more effectively: it decomposes the problem step by step, correctly deduces that each street has 20 houses, and thereby arrives at the correct total.

Question

In my neighborhood, there are six streets. There are 10 houses on each side of each street. No house faces two different streets. How many houses are in my neighborhood?

Ground Truth

120

Vanilla GRPO

To determine the total number of houses in the neighborhood, we can follow these steps:

1. **Identify the number of streets and houses per street:** - There are 6 streets. - Each street has 10 houses on each side.
2. **Calculate the number of houses on one street:** Since there are 10 houses on each side of a street, and each house faces only one street, the total number of houses on one street is 10 (since they are all on the same street).
3. **Calculate the total number of houses in the neighborhood:** There are 6 streets, and each street has 10 houses. Therefore, the total number of houses is $6 \times 10 = 60$.

Putting the final answer within \square , we get:

\square 60

GRPO with Auxiliary Shaping Term

To find the total number of houses in the neighborhood, let’s break down the problem step by step.

1. There are 6 streets in the neighborhood.
2. Each street has houses on both sides.
3. There are 10 houses on each side of every street.
4. No house faces two different streets, meaning each house is counted only once.

First, calculate the number of houses on one side of a single street:

$$10 \text{ houses/side}$$

Since there are houses on both sides of each street, multiply by 2:

$$10 \text{ houses/side} \times 2 \text{ sides/street} = 20 \text{ houses/street}$$

Now, since there are 6 streets, multiply the number of houses per street by the number of streets:

$$20 \text{ houses/street} \times 6 \text{ streets} = 120 \text{ houses}$$

So, the total number of houses in the neighborhood is

\square 120

Figure 13: Case study: Vanilla GRPO overlooks the constraint and infers 10 houses per street, while our method exploits it correctly and infers 20.

Case Study III. As shown in Fig. 14, the task concerns solving a differential equation under the constraint of finding a purely exponential solution rather than a general one. The model trained with vanilla GRPO overlooks this constraint and defaults to the generic procedure for obtaining the full solution. In contrast, the model trained with GRPO augmented by the auxiliary shaping term respects the constraint and produces the correct purely exponential answer. This case illustrates how the auxiliary shaping term enhances exploitation by enforcing adherence to problem-specific constraints.

F.2 CASE STUDY FOR PASS@16 SETTING

Case Study I. As shown in Fig. 15, the question is a simple elementary-level math problem requiring the integer solution $x \geq 1, x \neq 2$. While the vanilla GRPO model consistently outputs 3, which is incorrect, the model trained with the auxiliary shaping term produces 1 in 5 out of 16 roll-outs, the correct answer. This case highlights that the auxiliary shaping term enhances the model’s exploration ability, enabling it to consider a wider range of possibly valid solutions.

Question

Find a purely exponential solution of $\frac{d^4x}{dt^4} - x = e^{-2t}$.

Ground Truth

$$\frac{e^{-2t}}{15}$$

Vanilla GRPO

To find a purely exponential solution of the differential equation ($\frac{d^4x}{dt^4} - x = e^{-2t}$), we will follow these steps:

1. **Find the complementary solution by solving the homogeneous equation:**

$$\frac{d^4x}{dt^4} - x = 0$$

The characteristic equation is:

$$r^4 - 1 = 0$$

Solving for r , we get:

$$r^4 = 1 \implies r = \pm 1, \pm i$$

Therefore, the complementary solution is:

$$x_c(t) = C_1 e^t + C_2 e^{-t} + C_3 \cos(t) + C_4 \sin(t)$$

2. **Find a particular solution using the method of undetermined coefficients:**

Since the right-hand side of the non-homogeneous equation is e^{-2t} , we assume a particular solution of the form:

$$x_p(t) = A e^{-2t}$$

Taking the fourth derivative of $x_p(t)$:

$$\frac{d^4}{dt^4}(A e^{-2t}) = A(-2)^4 e^{-2t} = 16A e^{-2t}$$

Substituting $x_p(t)$ and its fourth derivative into the original differential equation:

$$16A e^{-2t} - A e^{-2t} = e^{-2t}$$

Simplifying, we get:

$$(16A - A)e^{-2t} = e^{-2t} \implies 15A e^{-2t} = e^{-2t}$$

Therefore:

$$15A = 1 \implies A = \frac{1}{15}$$

So, the particular solution is:

$$x_p(t) = \frac{1}{15} e^{-2t}$$

3. **Combine the complementary and particular solutions:**

The general solution to the differential equation is:

$$x(t) = x_c(t) + x_p(t) = C_1 e^t + C_2 e^{-t} + C_3 \cos(t) + C_4 \sin(t) + \frac{1}{15} e^{-2t}$$

Thus, the final answer is:

$$C_1 e^t + C_2 e^{-t} + C_3 \cos(t) + C_4 \sin(t) + \frac{1}{15} e^{-2t}$$

Figure 14: Case study: Vanilla GRPO ignores the constraint of a purely exponential solution, while our method enforces it and yields the correct result.

GRPO with Auxiliary Shaping Term

To find a purely exponential solution to the differential equation

$$\frac{d^4 x}{dt^4} - x = e^{-2t}$$

, we will follow these steps:

1. **Find the complementary solution by solving the homogeneous equation:**

$$\frac{d^4 x}{dt^4} - x = 0$$

The characteristic equation is:

$$r^4 - 1 = 0$$

Solving for r , we get:

$$r^4 = 1 \implies r = \pm 1, \pm i$$

Therefore, the complementary solution is:

$$x_c(t) = C_1 e^t + C_2 e^{-t} + C_3 \cos(t) + C_4 \sin(t)$$

2. **Find a particular solution using the method of undetermined coefficients:** Since the right-hand side of the non-homogeneous equation is e^{-2t} , we assume a particular solution of the form:

$$x_p(t) = A e^{-2t}$$

Taking the fourth derivative of $x_p(t)$:

$$\frac{d^4 x_p}{dt^4} = 16A e^{-2t}$$

Substituting $x_p(t)$ and its fourth derivative into the original differential equation:

$$16A e^{-2t} - A e^{-2t} = e^{-2t}$$

Simplifying, we get:

$$15A e^{-2t} = e^{-2t}$$

Solving for A :

$$15A = 1 \implies A = \frac{1}{15}$$

Therefore, the particular solution is:

$$x_p(t) = \frac{1}{15} e^{-2t}$$

3. **Combine the complementary and particular solutions:** The general solution to the differential equation is:

$$x(t) = x_c(t) + x_p(t) = C_1 e^t + C_2 e^{-t} + C_3 \cos(t) + C_4 \sin(t) + \frac{1}{15} e^{-2t}$$

Thus, the purely exponential solution is:

$$\boxed{\frac{1}{15} e^{-2t}}$$

Figure 14: Case study: Vanilla GRPO ignores the constraint of a purely exponential solution, while our method enforces it and yields the correct result (continued).

Question

Given $f(x) = \frac{\sqrt{x-1}}{x-2}$, what is the smallest possible integer value for x such that $f(x)$ has a real number value?

Ground Truth

1

Figure 15: Case study demonstrating improved exploration: the auxiliary shaping term enables the model to explore and reach the correct solution.

Vallina GRPO#1-#8

(Details omitted as they are not crucial for this case study.)

1. **Numerator Condition:** The numerator is $\sqrt{x-1}$. For the square root to be defined and result in a real number, the expression inside the square root must be non-negative.

$$x - 1 \geq 0 \implies x \geq 1$$

2. **Denominator Condition:** The denominator is $x - 2$. For the function to be defined, the denominator must not be zero.

$$x - 2 \neq 0 \implies x \neq 2$$

Combining these two conditions, we get:

$$x \geq 1 \text{ and } x \neq 2$$

The smallest integer that satisfies $x \geq 1$ and $x \neq 2$ is $x = 3$.

Therefore, the smallest possible integer value for x such that $f(x)$ has a real number value is $\boxed{3}$.

To determine the smallest possible integer value for x such that $f(x) = \frac{\sqrt{x-1}}{x-2}$ has a real number value, we need to ensure that both the numerator and the denominator satisfy their respective conditions for real numbers.

1. **Numerator Condition:** The expression inside the square root must be non-negative.

$$x - 1 \geq 0 \implies x \geq 1$$

2. **Denominator Condition:** The denominator must not be zero to avoid division by zero.

$$x - 2 \neq 0 \implies x \neq 2$$

Combining these conditions, we need $x \geq 1$ and $x \neq 2$. The smallest integer that satisfies these conditions is $x = 3$.

Therefore, the smallest possible integer value for x such that $f(x)$ has a real number value is $\boxed{3}$.

To determine the smallest possible integer value for x such that $f(x) = \frac{\sqrt{x-1}}{x-2}$ has a real number value, we need to ensure that both the numerator and the denominator satisfy certain conditions.

1. **Numerator Condition:** The expression inside the square root must be non-negative because the square root of a negative number is not a real number.

$$x - 1 \geq 0 \implies x \geq 1$$

2. **Denominator Condition:** The denominator must not be zero because division by zero is undefined.

$$x - 2 \neq 0 \implies x \neq 2$$

Combining these conditions, we get:

$$x \geq 1 \text{ and } x \neq 2$$

The smallest integer that satisfies $x \geq 1$ and $x \neq 2$ is $x = 3$.

(Details omitted as they are not crucial for this case study.)

1. **Square Root Condition:** The expression inside the square root, $x - 1$, must be greater than or equal to zero for the square root to be a real number.

$$x - 1 \geq 0 \implies x \geq 1$$

2. **Denominator Condition:** The denominator, $x - 2$, must not be zero to avoid division by zero.

$$x - 2 \neq 0 \implies x \neq 2$$

Combining these two conditions, we get:

$$x \geq 1 \text{ and } x \neq 2$$

The smallest integer that satisfies $x \geq 1$ and $x \neq 2$ is $x = 3$.

Therefore, the smallest possible integer value for x such that $f(x)$ has a real number value is $\boxed{3}$.

(Details omitted as they are not crucial for this case study.)

1. For the square root to be defined, the expression inside it must be greater than or equal to zero:

$$x - 1 \geq 0$$

Solving this inequality:

$$x \geq 1$$

2. For the denominator to be non-zero:

$$x - 2 \neq 0$$

Solving this equation:

$$x \neq 2$$

(Details omitted as they are not crucial for this case study.)

Therefore, the smallest possible integer value for x such that $f(x)$ has a real number value is:

$$\boxed{3}$$

(Details omitted as they are not crucial for this case study.)

1. For the square root to be defined, the expression inside it must be greater than or equal to zero:

$$x - 1 \geq 0$$

Solving this inequality:

$$x \geq 1$$

2. For the function to be defined, the denominator must not be zero:

$$x - 2 \neq 0$$

Solving this equation:

$$x \neq 2$$

(Details omitted as they are not crucial for this case study.)

Therefore, the smallest possible integer value for x such that $f(x)$ has a real number value is $\boxed{3}$.

(Details omitted as they are not crucial for this case study.)

1. For the square root to be defined, we need:

$$x - 1 \geq 0$$

Solving this inequality:

$$x \geq 1$$

2. For the denominator to be non-zero, we need:

$$x - 2 \neq 0$$

Solving this equation:

$$x \neq 2$$

Combining these two conditions, x must be greater than or equal to 1 but not equal to 2. The smallest integer that satisfies this condition is $x = 3$. Therefore, the smallest possible integer value for x such that $f(x)$ has a real number value is $\boxed{3}$.

(Details omitted as they are not crucial for this case study.)

1. **Square Root Condition:** The expression inside the square root, $x - 1$, must be greater than or equal to zero for the square root to be a real number.

$$x - 1 \geq 0 \implies x \geq 1$$

2. **Denominator Condition:** The denominator, $x - 2$, must not be zero to avoid division by zero.

$$x - 2 \neq 0 \implies x \neq 2$$

Combining these two conditions, we get:

$$x \geq 1 \text{ and } x \neq 2$$

The smallest integer that satisfies $x \geq 1$ and $x \neq 2$ is $x = 3$.

Therefore, the smallest possible integer value for x such that $f(x)$ has a real number value is $\boxed{3}$.

Figure 15: Case study demonstrating improved exploration: the auxiliary shaping term enables the model to explore and reach the correct solution (continued).

Vanilla GRPO#9-#16

(Details omitted as they are not crucial for this case study.)

1. Numerator Condition: The expression inside the square root, $x-1$, must be non-negative because the square root of a negative number is not a real number. Therefore, we need:

$$x-1 \geq 0 \implies x \geq 1$$

2. Denominator Condition: The denominator, $x-2$, must not be zero because division by zero is undefined. Therefore, we need:

$$x-2 \neq 0 \implies x \neq 2$$

Combining these two conditions, we get:

$$x \geq 1 \text{ and } x \neq 2$$

The smallest integer that satisfies $x \geq 1$ and $x \neq 2$ is $x = 3$.

Therefore, the smallest possible integer value for x such that $f(x)$ has a real number value is: $\boxed{3}$

(Details omitted as they are not crucial for this case study.)

1. Numerator Condition: The expression inside the square root, $x-1$, must be non-negative because the square root of a negative number is not a real number. Therefore, we need:

$$x-1 \geq 0 \implies x \geq 1$$

2. Denominator Condition: The denominator, $x-2$, must not be zero because division by zero is undefined. Therefore, we need:

$$x-2 \neq 0 \implies x \neq 2$$

Combining these two conditions, we get:

$$x \geq 1 \text{ and } x \neq 2$$

The smallest integer that satisfies $x \geq 1$ and $x \neq 2$ is $x = 3$.

Therefore, the smallest possible integer value for x such that $f(x)$ has a real number value is $\boxed{3}$.

(Details omitted as they are not crucial for this case study.)

1. For the square root to be defined, we need:

$$x-1 \geq 0$$

$$x \geq 1$$

2. For the denominator to be non-zero, we need:

$$x-2 \neq 0$$

$$x \neq 2$$

Combining these two conditions, we get:

$$x \geq 1$$

$$x \neq 2$$

The smallest integer that satisfies $x \geq 1$ and $x \neq 2$ is $x = 3$.

Therefore, the smallest possible integer value for x such that $f(x)$ has a real number value is $\boxed{3}$.

(Details omitted as they are not crucial for this case study.)

1. Numerator Condition: The expression under the square root, $x-1$, must be non-negative because the square root of a negative number is not a real number. Therefore, we need:

$$x-1 \geq 0 \implies x \geq 1$$

2. Denominator Condition: The denominator, $x-2$, must not be zero because division by zero is undefined. Therefore, we need:

$$x-2 \neq 0 \implies x \neq 2$$

Combining these two conditions, we get:

$$x \geq 1 \text{ and } x \neq 2$$

The smallest integer that satisfies $x \geq 1$ and $x \neq 2$ is $x = 3$.

Therefore, the smallest possible integer value for x such that $f(x)$ has a real number value is: $\boxed{3}$

(Details omitted as they are not crucial for this case study.)

1. Numerator Condition: The numerator is $\sqrt{x-1}$. For the square root to be defined and result in a real number, the expression inside the square root must be non-negative.

$$x-1 \geq 0 \implies x \geq 1$$

2. Denominator Condition: The denominator is $x-2$. For the function to be defined, the denominator must not be zero.

$$x-2 \neq 0 \implies x \neq 2$$

Combining these two conditions, we need x to be greater than or equal to 1, but not equal to 2. Therefore, the smallest possible integer value for x that satisfies both conditions is

$$\boxed{3}$$

(Details omitted as they are not crucial for this case study.)

1. Square Root Condition: The expression inside the square root, $x-1$, must be greater than or equal to zero for the square root to be a real number.

$$x-1 \geq 0 \implies x \geq 1$$

2. Denominator Condition: The denominator, $x-2$, must not be zero to avoid division by zero.

$$x-2 \neq 0 \implies x \neq 2$$

Combining these two conditions, we get:

$$x \geq 1 \text{ and } x \neq 2$$

The smallest integer that satisfies $x \geq 1$ and $x \neq 2$ is $x = 3$.

Therefore, the smallest possible integer value for x such that $f(x)$ has a real number value is $\boxed{3}$.

To determine the smallest possible integer value for x such that $f(x) = \frac{\sqrt{x-1}}{x-2}$ has a real number value, we need to ensure that both the numerator and the denominator satisfy their respective conditions for real numbers.

1. Numerator Condition: The expression inside the square root must be non-negative.

$$x-1 \geq 0 \implies x \geq 1$$

2. Denominator Condition: The denominator must not be zero.

$$x-2 \neq 0 \implies x \neq 2$$

Combining these conditions, we need x to be greater than or equal to 1 but not equal to 2. Therefore, the smallest possible integer value for x that satisfies both conditions is

$$\boxed{3}$$

(Details omitted as they are not crucial for this case study.)

1. Numerator Condition: The numerator is $\sqrt{x-1}$. For the square root to be a real number, the expression inside the square root must be non-negative.

$$x-1 \geq 0 \implies x \geq 1$$

2. Denominator Condition: The denominator is $x-2$. For the function to be defined, the denominator must not be zero.

$$x-2 \neq 0 \implies x \neq 2$$

Combining these two conditions, we get:

$$x \geq 1 \text{ and } x \neq 2$$

The smallest integer that satisfies $x \geq 1$ and $x \neq 2$ is $x = 3$.

Therefore, the smallest possible integer value for x such that $f(x)$ has a real number value is $\boxed{3}$.

Figure 15: Case study demonstrating improved exploration: the auxiliary shaping term enables the model to explore and reach the correct solution (continued).

GRPO with Auxiliary Shaping Term#1-#8

(Details omitted as they are not crucial for this case study.)

1. Numerator Condition: The numerator is $\sqrt{x-1}$. For the square root to be defined and real, the expression inside the square root must be non-negative.

$$x-1 \geq 0 \implies x \geq 1$$

2. Denominator Condition: The denominator is $x-2$. For the function to be defined, the denominator must not be zero.

$$x-2 \neq 0 \implies x \neq 2$$

Combining these conditions, we need x to be greater than or equal to 1, but not equal to 2. The smallest integer that satisfies these conditions is $x = 3$.

Therefore, the smallest possible integer value for x such that $f(x)$ has a real number value is $\boxed{3}$.

(Details omitted as they are not crucial for this case study.)

1. For the square root to be defined in the real numbers, the expression inside it must be greater than or equal to zero:

$$x-1 \geq 0$$

Solving this inequality:

$$x \geq 1$$

2. For the function to be defined, the denominator must not be zero:

$$x-2 \neq 0$$

Solving this equation:

$$x \neq 2$$

(Details omitted as they are not crucial for this case study.)

Thus, the smallest possible integer value for x such that $f(x)$ has a real number value is $\boxed{3}$.

(Details omitted as they are not crucial for this case study.)

1. The expression inside the square root must be non-negative. 2. The denominator must not be zero.

(Details omitted as they are not crucial for this case study.)

Step 3: Combine the conditions From Step 1, we know $x \geq 1$. From Step 2, we know $x \neq 2$. Therefore, the smallest integer value for x that satisfies both conditions is the smallest integer greater than 1, which is 3.

Final Answer The smallest possible integer value for x such that $f(x)$ has a real number value is

$$\boxed{3}.$$

(Details omitted as they are not crucial for this case study.)

Combining the Conditions From Condition 1, we have $x \geq 1$. From Condition 2, we have $x \neq 2$.

Combining these, the smallest integer value for x that satisfies both conditions is $x = 3$.

Verification Let's verify that $x = 3$ works: - For $x = 3$, $\sqrt{x-1} = \sqrt{3-1} = \sqrt{2}$, which is a real number. - The denominator $x-2 = 3-2 = 1$, which is not zero.

Since both conditions are satisfied, the smallest possible integer value for x is indeed 3.

Thus, the final answer is:

$$\boxed{3}$$

(Details omitted as they are not crucial for this case study.)

1. Numerator Condition: The expression under the square root, $x-1$, must be non-negative because the square root of a negative number is not a real number. Therefore, we need:

$$x-1 \geq 0 \implies x \geq 1$$

2. Denominator Condition: The denominator, $x-2$, must not be zero because division by zero is undefined. Therefore, we need:

$$x-2 \neq 0 \implies x \neq 2$$

Combining these two conditions, we get:

$$x \geq 1 \text{ and } x \neq 2$$

The smallest integer that satisfies $x \geq 1$ but not $x = 2$ is $x = 1$.

Therefore, the smallest possible integer value for x such that $f(x)$ has a real number value is $\boxed{1}$.

(Details omitted as they are not crucial for this case study.)

Combining the Conditions From Condition 1, we know $x \geq 1$. From Condition 2, we know $x \neq 2$.

The smallest integer that satisfies $x \geq 1$ but not $x = 2$ is $x = 1$.

(Details omitted as they are not crucial for this case study.)

Since $f(1)$ is a real number, $x = 1$ is indeed a valid solution.

Therefore, the smallest possible integer value for x such that $f(x)$ has a real number value is $\boxed{1}$.

(Details omitted as they are not crucial for this case study.)

1. For $\sqrt{x-1}$ to be defined, we need:

$$x-1 \geq 0 \implies x \geq 1$$

2. For the denominator $x-2$ to be non-zero, we need:

$$x-2 \neq 0 \implies x \neq 2$$

Combining these two conditions, we get:

$$x \geq 1 \text{ and } x \neq 2$$

The smallest integer that satisfies $x \geq 1$ and $x \neq 2$ is $x = 1$.

(Details omitted as they are not crucial for this case study.)

Since $f(1) = 0$ is a real number, our solution is confirmed.

Therefore, the smallest possible integer value for x such that $f(x)$ has a real number value is $\boxed{1}$.

(Details omitted as they are not crucial for this case study.)

1. For $\sqrt{x-1}$ to be defined in the real numbers, we need:

$$x-1 \geq 0 \implies x \geq 1$$

2. For the denominator $x-2$ to not be zero, we need:

$$x-2 \neq 0 \implies x \neq 2$$

Combining these two conditions, x must be greater than or equal to 1 but not equal to 2. The smallest integer that satisfies this condition is $x = 1$.

Therefore, the smallest possible integer value for x such that $f(x)$ has a real number value is $\boxed{3}$.

Figure 15: Case study demonstrating improved exploration: the auxiliary shaping term enables the model to explore and reach the correct solution (continued).

GRPO with Auxiliary Shaping Term#9-#16

(Details omitted as they are not crucial for this case study.)

1. **Numerator Condition:** The expression inside the square root, $x-1$, must be non-negative because the square root of a negative number is not a real number. Therefore, we need:

$$x-1 \geq 0 \implies x \geq 1$$

2. **Denominator Condition:** The denominator, $x-2$, must not be zero because division by zero is undefined. Therefore, we need:

$$x-2 \neq 0 \implies x \neq 2$$

Combining these two conditions, we get:

$$x \geq 1 \text{ and } x \neq 2$$

The smallest integer that satisfies $x \geq 1$ and $x \neq 2$ is $x = 1$.

Therefore, the smallest possible integer value for x such that $f(x)$ has a real number value is $\boxed{1}$.

(Details omitted as they are not crucial for this case study.)

1. **Numerator Condition:** The expression under the square root must be non-negative.

$$x-1 \geq 0 \implies x \geq 1$$

2. **Denominator Condition:** The denominator must not be zero.

$$x-2 \neq 0 \implies x \neq 2$$

Combining these two conditions, we get:

$$x \geq 1 \text{ and } x \neq 2$$

The smallest integer that satisfies $x \geq 1$ and $x \neq 2$ is $x = 3$.

Therefore, the smallest possible integer value for x such that $f(x)$ has a real number value is $\boxed{3}$.

(Details omitted as they are not crucial for this case study.)

1. **Numerator Condition:** The expression inside the square root must be non-negative.

$$x-1 \geq 0 \implies x \geq 1$$

This ensures that $\sqrt{x-1}$ is a real number.

2. **Denominator Condition:** The denominator must not be zero.

$$x-2 \neq 0 \implies x \neq 2$$

This ensures that the function is defined. Combining these two conditions, we get:

$$x \geq 1 \text{ and } x \neq 2$$

The smallest integer that satisfies $x \geq 1$ and $x \neq 2$ is $x = 3$.

Therefore, the smallest possible integer value for x such that $f(x)$ has a real number value is $\boxed{3}$.

(Details omitted as they are not crucial for this case study.)

1. For the square root to be defined, we need:

$$x-1 \geq 0$$

Solving this inequality:

$$x \geq 1$$

2. For the denominator to be non-zero, we need:

$$x-2 \neq 0$$

Solving this equation:

$$x \neq 2$$

Combining these two conditions, x must be greater than or equal to 1 but not equal to 2. The smallest integer that satisfies this condition is $x = 3$.

Therefore, the smallest possible integer value for x such that $f(x)$ has a real number value is $\boxed{3}$.

(Details omitted as they are not crucial for this case study.)

1. The expression inside the square root must be non-negative. 2. The denominator must not be zero.

Let's address these conditions one by one:

1. For the square root to be defined, the expression inside it must be greater than or equal to zero:

$$x-1 \geq 0 \implies x \geq 1$$

2. For the denominator to be non-zero:

$$x-2 \neq 0 \implies x \neq 2$$

Combining these conditions, we need x to be greater than or equal to 1 but not equal to 2. The smallest integer that satisfies this is $x = 3$.

Therefore, the smallest possible integer value for x such that $f(x)$ has a real number value is $\boxed{3}$.

(Details omitted as they are not crucial for this case study.)

1. **Numerator Condition:** The expression inside the square root must be non-negative because the square root of a negative number is not a real number.

$$x-1 \geq 0 \implies x \geq 1$$

2. **Denominator Condition:** The denominator must not be zero because division by zero is undefined.

$$x-2 \neq 0 \implies x \neq 2$$

Combining these two conditions, we get:

$$x \geq 1 \text{ and } x \neq 2$$

The smallest integer that satisfies $x \geq 1$ and $x \neq 2$ is $x = 3$.

Therefore, the smallest possible integer value for x such that $f(x)$ has a real number value is $\boxed{3}$.

(Details omitted as they are not crucial for this case study.)

1. **Numerator Condition:** The expression under the square root, $x-1$, must be non-negative because the square root of a negative number is not a real number.

$$x-1 \geq 0 \implies x \geq 1$$

2. **Denominator Condition:** The denominator, $x-2$, must not be zero because division by zero is undefined.

$$x-2 \neq 0 \implies x \neq 2$$

Combining these conditions, we need $x \geq 1$ and $x \neq 2$. The smallest integer that satisfies these conditions is $x = 1$.

(Details omitted as they are not crucial for this case study.)

Therefore, the smallest possible integer value for x such that $f(x)$ has a real number value is $\boxed{1}$.

To determine the smallest possible integer value for x such that $f(x) = \frac{\sqrt{x-1}}{x-2}$ has a real number value, we need to ensure that both the numerator and the denominator satisfy their respective conditions for real numbers.

1. **Numerator Condition:** The expression inside the square root must be non-negative.

$$x-1 \geq 0 \implies x \geq 1$$

2. **Denominator Condition:** The denominator must not be zero.

$$x-2 \neq 0 \implies x \neq 2$$

Combining these conditions, we need x to be greater than or equal to 1 but not equal to 2. The smallest integer that satisfies this condition is $x = 3$.

Therefore, the smallest possible integer value for x such that $f(x)$ has a real number value is $\boxed{3}$.

Figure 15: Case study demonstrating improved exploration: the auxiliary shaping term enables the model to explore and reach the correct solution (continued).

Case Study II. As shown in Fig. 16, this high-school level geometry problem illustrates the contrast between vanilla GRPO and GRPO with the auxiliary shaping term. The vanilla GRPO model fails to produce the correct answer in any rollout. In contrast, the model trained with the auxiliary shaping term succeeds in 5 out of 16 rollouts. Moreover, its reasoning traces display higher exploratory diversity: it applies the law of sines 9 times, the law of cosines 4 times, and other general geometric properties 3 times. By comparison, the vanilla GRPO model relies more narrowly on the law of sines (11 times), with only limited use of other strategies. This case highlights that the auxiliary shaping term enhances the model’s exploration capacity, enabling it to leverage a broader range of problem-solving strategies rather than over-committing to a single path.

Question

Abdul and Chiang are standing 48 feet apart in a field. Bharat is standing in the same field as far from Abdul as possible so that the angle formed by his lines of sight to Abdul and Chiang measures 60° . What is the square of the distance (in feet) between Abdul and Bharat?

Ground Truth

3072

Vanilla GRPO#1-#8

(Details omitted as they are not crucial for this case study.)

1. Identify the triangle and its properties:

(Details omitted as they are not crucial for this case study.)

2. Use the Law of Sines:

(Details omitted as they are not crucial for this case study.)

3. Apply the Law of Sines:

(Details omitted as they are not crucial for this case study.)

4. Find the square of the distance:

(Details omitted as they are not crucial for this case study.)

Therefore, the square of the distance between Abdul and Bharat is $\boxed{2304}$.

To solve this problem, we can use the Law of Sines in trigonometry. Let's denote the distance between Abdul and Bharat as x and the distance between Chiang and Bharat as y . We know that the angle between Abdul and Chiang as seen from Bharat is 60° , and the distance between Abdul and Chiang is 48 feet.

Given: $\angle ABC = 60^\circ$
 $AB = 48$ feet - We need to find x^2

First, we apply the Law of Sines in triangle ABC :
 (Details omitted as they are not crucial for this case study.)

Thus, the square of the distance between Abdul and Bharat is $\boxed{9216}$.

To solve this problem, we can use the Law of Sines in trigonometry. Let's denote the distance between Abdul and Bharat as AB , and the distance between Chiang and Bharat as BC . Since Bharat is as far from Abdul as possible to form a 60° angle, triangle ABC is a right triangle with the right angle at Chiang. This means $\angle ACB = 90^\circ$ and $\angle BAC = 60^\circ$.

(Details omitted as they are not crucial for this case study.)

Thus, the square of the distance between Abdul and Bharat is $\boxed{9216}$.

First, we need to find the distance AB using the Law of Sines. In triangle ABC :

(Details omitted as they are not crucial for this case study.)

Now, we need to find the square of the distance AB :

(Details omitted as they are not crucial for this case study.)

Thus, the square of the distance between Abdul and Bharat is $\boxed{1728}$.

To verify the accuracy of this result, we can use Python to perform the calculations.

(Details omitted as they are not crucial for this case study.)

To solve this problem, we can use the Law of Sines and some geometric properties. Let's break it down step by step.

1. Identify the triangle and its properties:

(Details omitted as they are not crucial for this case study.)

2. Apply the Law of Sines:

(Details omitted as they are not crucial for this case study.)

3. Calculate the distances:

(Details omitted as they are not crucial for this case study.)

4. Find the square of the distance:

(Details omitted as they are not crucial for this case study.)

So, the square of the distance between Abdul and Bharat is $\boxed{768}$.

(Details omitted as they are not crucial for this case study.)

1. Recognize that the triangle ABC is a right triangle with $\angle BAC = 90^\circ$ and $\angle ABC = 60^\circ$. Therefore, $\angle ACB = 30^\circ$.

(Details omitted as they are not crucial for this case study.)

3. Since $AC = 48$ feet, and in a 30-60-90 triangle, the side opposite the 60° angle is $\sqrt{3}$ times the side opposite the 30° angle, we can find AB :

$$AB = 48\sqrt{3}$$

(Details omitted as they are not crucial for this case study.)

Therefore, the square of the distance between Abdul and Bharat is $\boxed{6912}$ feet.

To solve this problem, we need to use some geometric principles, specifically involving the Law of Sines and properties of triangles.

1. Identify the triangle and the given information:

(Details omitted as they are not crucial for this case study.)

2. Use the Law of Sines to find the distance BC (the distance from Bharat to Chiang):

(Details omitted as they are not crucial for this case study.)

3. Find the distance AC (the distance from Abdul to Bharat):

(Details omitted as they are not crucial for this case study.)

Therefore, the square of the distance between Abdul and Bharat is $\boxed{11520}$.

(Details omitted as they are not crucial for this case study.)

1. Identify the triangle and the given information:

(Details omitted as they are not crucial for this case study.)

2. Use the Law of Sines:

(Details omitted as they are not crucial for this case study.)

3. Maximize AB:

(Details omitted as they are not crucial for this case study.)

4. Apply the Pythagorean theorem:

(Details omitted as they are not crucial for this case study.)

Thus, the square of the distance between Abdul and Bharat is $\boxed{9216}$.

Figure 16: Case study: Geometry problem. GRPO with auxiliary shaping term not only achieves higher accuracy but also explores more diverse reasoning strategies than vanilla GRPO.

Vanilla GRPO#9-#16

To solve this problem, we can use the Law of Sines and some geometric properties. Let's break it down step by step.

1. Identify the triangle and the given information:

(Details omitted as they are not crucial for this case study.)

2. Determine the largest possible angle at A:

(Details omitted as they are not crucial for this case study.)

3. Use the Pythagorean theorem:

(Details omitted as they are not crucial for this case study.)

4. Find the square of the distance between Abdul and Bharat:

(Details omitted as they are not crucial for this case study.)

So, the square of the distance between Abdul and Bharat is $\boxed{9216}$.

To solve this problem, we can use some geometric properties and trigonometry. Let's break it down step by step:

1. Identify the triangle formed:

(Details omitted as they are not crucial for this case study.)

2. Use the Law of Sines:

(Details omitted as they are not crucial for this case study.)

3. Maximize the distance:

(Details omitted as they are not crucial for this case study.)

4. Square the distance:

(Details omitted as they are not crucial for this case study.)

Let's calculate it:

$$48^2 = 2304$$

So, the square of the distance between Abdul and Bharat is $\boxed{2304}$.

To solve the problem, we need to determine the distance between Abdul and Bharat, given that the angle between their lines of sight to Chiang is 60° and that Bharat is positioned to be as far from Abdul as possible.

(Details omitted as they are not crucial for this case study.)

Using the Law of Cosines in triangle ABC :

(Details omitted as they are not crucial for this case study.)

$$BC^2 = d^2 + 2304 - 48d$$

(Details omitted as they are not crucial for this case study.)

The square of the distance between Abdul and Bharat is:

$$d^2 = 96^2 = 9216$$

Thus, the square of the distance between Abdul and Bharat is $\boxed{9216}$.

(Details omitted as they are not crucial for this case study.)

1. Identify the known values:

(Details omitted as they are not crucial for this case study.)

2. Set up the triangle:

(Details omitted as they are not crucial for this case study.)

3. Apply the Law of Sines:

(Details omitted as they are not crucial for this case study.)

4. Determine the angles:

(Details omitted as they are not crucial for this case study.)

5. Simplify the Law of Sines equation:

(Details omitted as they are not crucial for this case study.)

Therefore, the square of the distance between Abdul and Bharat is $\boxed{2304}$.

To solve this problem, we need to use some geometric properties and trigonometry. Let's break it down step by step.

1. Understanding the Problem:

(Details omitted as they are not crucial for this case study.)

2. Geometric Insight:

(Details omitted as they are not crucial for this case study.)

3. Using Trigonometry:

(Details omitted as they are not crucial for this case study.)

4. Calculating the Distance: - Let the distance AB be x . Since $\angle ABC$ is 60° and we need to maximize AB, we use the Law of Cosines in triangle ABC:

(Details omitted as they are not crucial for this case study.)

Therefore, the square of the distance between Abdul and Bharat is $\boxed{432}$.

(Details omitted as they are not crucial for this case study.)

1. Identify the given information:

(Details omitted as they are not crucial for this case study.)

2. Visualize the problem:

(Details omitted as they are not crucial for this case study.)

3. Use the Law of Sines:

(Details omitted as they are not crucial for this case study.)

4. Properties of an equilateral triangle:

(Details omitted as they are not crucial for this case study.)

5. Calculate the square of the distance:

(Details omitted as they are not crucial for this case study.)

Thus, the square of the distance between Abdul and Bharat is $\boxed{2304}$.

Providethefinalanswerwithin

To solve this problem, we need to use some geometric properties and trigonometry. Let's break it down step by step.

1. Understand the Problem:

(Details omitted as they are not crucial for this case study.)

2. Visualize the Problem:

(Details omitted as they are not crucial for this case study.)

3. Use Geometric Properties:

(Details omitted as they are not crucial for this case study.)

4. Apply Trigonometry:

(Details omitted as they are not crucial for this case study.)

5. Calculate the Distance:

- $AB = 2 * AC = 2 * 48 = 96$ feet. - The square of the distance AB is 96^2 .

6. Final Calculation:

- $96^2 = 9216$.

So, the square of the distance between Abdul and Bharat is $\boxed{9216}$.

To solve this problem, we can use the Law of Sines in trigonometry. Let's break it down step by step:

1. Identify the given information:

(Details omitted as they are not crucial for this case study.)

2. Set up the triangle:

(Details omitted as they are not crucial for this case study.)

3. Use the Law of Sines:

(Details omitted as they are not crucial for this case study.)

4. Find the square of the distance:

The distance between Abdul and Bharat is 24 feet. The square of this distance is:

$$24^2 = 576$$

Therefore, the square of the distance between Abdul and Bharat is $\boxed{576}$.

Figure 16: Case study: Geometry problem. GRPO with auxiliary shaping term not only achieves higher accuracy but also explores more diverse reasoning strategies than vanilla GRPO (continued).

GRPO with Auxiliary Shaping Term#1-#8

(Details omitted as they are not crucial for this case study.)

Given that $\angle ABC = 60^\circ$ and $AC = 48$ feet, we can use the Law of Sines to find AB :
(Details omitted as they are not crucial for this case study.)

The square of the distance AB is:

$$(32\sqrt{3})^2 = 32^2 \times 3 = 1024 \times 3$$

Thus, the square of the distance between Abdul and Bharat is $\boxed{3072}$.

To solve this problem, we can use the Law of Sines in trigonometry.

(Details omitted as they are not crucial for this case study.)

Given that $AC = 48$ feet, we can use the Law of Sines to find AB :

$$\frac{AB}{\sin(60^\circ)} = \frac{AC}{\sin(30^\circ)}$$

(Details omitted as they are not crucial for this case study.)

Solving for AB :

$$AB = 96 \times \frac{\sqrt{3}}{2} = 48\sqrt{3}$$

(Details omitted as they are not crucial for this case study.)

Therefore, the square of the distance between Abdul and Bharat is $\boxed{6912}$.

(Details omitted as they are not crucial for this case study.)

1. Identify the given information:

(Details omitted as they are not crucial for this case study.)

2. Visualize the problem:
(Details omitted as they are not crucial for this case study.)

3. Determine the type of triangle: - Since angle ABC and angle ACB are both 60° , triangle ABC is an equilateral triangle. In an equilateral triangle, all sides are equal.

4. Calculate the side length of the equilateral triangle: - Since $AC = 48$ feet and triangle ABC is equilateral, AB (the distance from Abdul to Bharat) is also 48 feet.
(Details omitted as they are not crucial for this case study.)

So, the square of the distance between Abdul and Bharat is $\boxed{2304}$.

To solve this problem, we can use the Law of Sines and some geometric properties. Let's denote the positions of Abdul, Chiang, and Bharat as points A , C , and B respectively. The distance between A and C is given as 48 feet. The angle $\angle ACB$ is 60° . We need to find the square of the distance AB , which is the farthest distance Bharat can be from Abdul.

(Details omitted as they are not crucial for this case study.)

Therefore, the square of the distance between Abdul and Bharat is $\boxed{6912}$.

To solve this problem, we need to use some geometric principles. Let's denote the positions of Abdul, Chiang, and Bharat as points A , C , and B respectively. We are given that the distance between A and C (AC) is 48 feet, and the angle ABC is 60° . We need to find the distance between A and B (AB), and then square it.
(Details omitted as they are not crucial for this case study.)

Step 3: Recognize that if triangle ABC is equilateral, then all sides are equal. Therefore, $AB = BC = AC = 48$ feet.
Step 4: Calculate the square of the distance AB . Since $AB = 48$ feet, we square this value to get AB^2 .

$$AB^2 = 48^2 = 2304$$

So, the square of the distance between Abdul and Bharat is $\boxed{2304}$.

To find the square of the distance between Abdul and Bharat, we can use the Law of Sines in trigonometry. Let's denote the distance between Abdul and Bharat as AB , and the distance between Chiang and Bharat as BC . Since Bharat is as far from Abdul as possible, triangle ABC is a right triangle with $\angle ACB = 90^\circ$.

Given: - $\angle ABC = 60^\circ$
- $AC = 48$ feet
We want to find AB^2 .
First, we apply the Law of Sines in triangle ABC :
(Details omitted as they are not crucial for this case study.)

Thus, the square of the distance between Abdul and Bharat is $\boxed{3072}$.

(Details omitted as they are not crucial for this case study.)

In a right triangle, if one of the angles is 60° , the triangle is a 30-60-90 triangle. In a 30-60-90 triangle, the sides are in the ratio $1 : \sqrt{3} : 2$. Here, AC is the hypotenuse, so we can set up the relationship as follows:

$$AC = 2 \times AB$$

$$48 = 2 \times AB$$

$$AB = \frac{48}{2} = 24 \text{ feet}$$

We need to find the square of the distance AB :

$$AB^2 = 24^2 = 576$$

Thus, the square of the distance between Abdul and Bharat is $\boxed{576}$.

(Details omitted as they are not crucial for this case study.)

Using the properties of a 30-60-90 triangle, we know that the side opposite the 60° angle is $\sqrt{3}$ times the side opposite the 30° angle. Let's denote the side opposite the 30° angle (which is half the distance between Abdul and Chiang) as x . Therefore, $AB = x\sqrt{3}$ and $BC = 2x$.

(Details omitted as they are not crucial for this case study.)

$$AB^2 = 2304(21 - 12\sqrt{3})$$

Since we are asked to find the square of the distance, and we have already calculated it, we can box the final answer:

$$\boxed{2304}$$

Figure 16: Case study: Geometry problem. GRPO with auxiliary shaping term not only achieves higher accuracy but also explores more diverse reasoning strategies than vanilla GRPO (continued).

GRPO with Auxiliary Shaping Term#9-#16

To solve this problem, we can use the Law of Sines in trigonometry.

(Details omitted as they are not crucial for this case study.)

Using the Law of Sines:

$$\frac{AB}{\sin(120^\circ)} = \frac{AC}{\sin(60^\circ)}$$

(Details omitted as they are not crucial for this case study.)

Therefore, the square of the distance between Abdul and Bharat is $\boxed{3072}$.

To solve this problem, we need to use some geometric properties and trigonometric relationships. Let's break it down step by step.

1. Identify the given information:

(Details omitted as they are not crucial for this case study.)

2. Visualize the problem:

(Details omitted as they are not crucial for this case study.)

3. Use the Law of Cosines:

(Details omitted as they are not crucial for this case study.)

4. Apply the Law of Cosines:

(Details omitted as they are not crucial for this case study.)

5. Find the square of the distance:

- The square of the distance between Abdul and Bharat is $d^2 = 2304$.

Therefore, the square of the distance between Abdul and Bharat is $\boxed{2304}$.

To solve this problem, we can use the Law of Sines and some geometric properties.

(Details omitted as they are not crucial for this case study.)

Given that the angle ABC is 60° and AB is maximized, the triangle ABC is a right triangle with angle ACB being 90° (since the angle at Bharat is 60° and the sum of angles in a triangle is 180° , the remaining angle at A must be 30° , making AB the hypotenuse of a 30-60-90 triangle).

(Details omitted as they are not crucial for this case study.)

Therefore, the square of the distance between Abdul and Bharat is $\boxed{3072}$.

To solve this problem, we need to use some geometric principles. Let's denote the positions of Abdul, Chiang, and Bharat as points A, C, and B respectively. The distance between A and C is 48 feet, and we need to find the distance AB when the angle $\angle ABC$ is 60° and B is as far from A as possible.

1. Identify the configuration:

(Details omitted as they are not crucial for this case study.)

2. Use the Law of Cosines:

(Details omitted as they are not crucial for this case study.)

3. Substitute into the Law of Cosines:

(Details omitted as they are not crucial for this case study.)

So, the square of the distance between Abdul and Bharat is $\boxed{3840}$ square feet.

To solve this problem, we need to use some geometric principles, specifically involving the Law of Sines and properties of triangles. Let's break it down step by step:

1. Identify the given information:

(Details omitted as they are not crucial for this case study.)

2. Visualize the problem:

(Details omitted as they are not crucial for this case study.)

3. Use the Law of Sines:

(Details omitted as they are not crucial for this case study.)

4. Determine the angles:

(Details omitted as they are not crucial for this case study.)

5. Calculate the distance AB:

(Details omitted as they are not crucial for this case study.)

Therefore, the square of the distance between Abdul and Bharat is $\boxed{3072}$.

To find the square of the distance between Abdul and Bharat, let's denote the distance between Abdul and Bharat as d , and the distance between Chiang and Bharat as d' .

Since the angle formed by the lines of sight to Abdul and Chiang is 60° , we can use the Law of Cosines in the triangle formed by Abdul, Chiang, and Bharat. The Law of Cosines states that for any triangle with sides a , b , and c , and the angle θ opposite side c :

$$c^2 = a^2 + b^2 - 2ab \cos(\theta)$$

(Details omitted as they are not crucial for this case study.)

Therefore, the square of the distance between Abdul and Bharat is $\boxed{2304}$.

To solve this problem, we'll use some geometric principles, particularly the Law of Sines and properties of triangles. Let's break down the problem step-by-step:

1. Identify the given information:

(Details omitted as they are not crucial for this case study.)

2. Visualize the problem:

(Details omitted as they are not crucial for this case study.)

3. Use the Law of Sines:

(Details omitted as they are not crucial for this case study.)

4. Apply the Law of Sines:

(Details omitted as they are not crucial for this case study.)

5. Use trigonometry in the right triangle:

(Details omitted as they are not crucial for this case study.)

Therefore, the square of the distance between Abdul and Bharat is $\boxed{1728}$.

To solve this problem, we need to use some geometric properties and trigonometry. Let's denote the positions of Abdul, Chiang, and Bharat as points A, C, and B respectively in the field. We know that AC = 48 feet and the angle $\angle ACB = 60^\circ$. We want to find the distance AB, which we'll denote as d , and then find d^2 .

1. Identify the type of triangle:

(Details omitted as they are not crucial for this case study.)

2. Apply the Law of Cosines:

(Details omitted as they are not crucial for this case study.)

3. Maximize the distance d:

(Details omitted as they are not crucial for this case study.)

Therefore, the square of the distance between Abdul and Bharat is $\boxed{1728}$.

Figure 16: Case study: Geometry problem. GRPO with auxiliary shaping term not only achieves higher accuracy but also explores more diverse reasoning strategies than vanilla GRPO (continued).